METABOLIC ENGINEERING OF *S. CEREVISIAE* FOR CAROTENOID PRODUCTION OPTIMIZATION

A Thesis

by

MICHELLE LYNN OLSON

Submitted to the Office of Graduate and Professional Studies of
Texas A&M University
in partial fulfillment of the requirements for the degree of

MASTER OF SCIENCE

Chair of Committee,	Katy C. Kao
Committee Members,	Arul Jayaraman
	Joshua Yuan
Head of Department,	M. Nazmul Karim

December 2014

Major Subject: Chemical Engineering

ABSTRACT

Isoprenoids are naturally produced compounds in the budding yeast *Saccharomyces cerevisiae*. They are involved in essential cellular functions of the cell and are also further synthesized into pharmaceuticals, carotenoids, and biofuel alternatives. *S. cerevisiae* is a key model eukaryotic organism because it is both tractable and a nonpathogenic GRAS organism (Generally Recognized As Safe). *S. cerevisiae* is used extensively in metabolic engineering due to its well-curated and annotated genome and the wide range of tools available for genetic modifications. Engineering *S. cerevisiae* for production of heterologous isoprenoid compounds is a sustainable and cost effective alternate to production via chemical synthesis. β-carotene, an abundant isoprenoid compound in nature, protects cells from oxidative stress and reactive oxidative species in the environment. Through a novel adaptive evolution experiment of *S. cerevisiae* with oxidative stress as the driving force, we obtained a carotenoid hyper-producer strain that is able to produce 18 ± 1 mg/g [dry cell weight] β-carotene in 3 ml cultures. To test the potential for scale-up β-carotene production in yeast, we fermented the cultures in a 7L bioreactor. Optimization of the bioreactor parameters revealed the influence of media composition, aeration, and pH on β-carotene production.

We aimed to further optimize β-carotene production in *S. cerevisiae* with genetic and metabolic engineering. We reintroduced the cytosolic catalase T (CTT1) gene and overexpressed the known bottleneck of the isoprenoid biosynthesis pathway, HMG1.

The reintroduction of CTT1 into SM14 (carotenoid hyper-producer) demonstrated improvement in carotenoid production, where production increased from 15 ± 3.3 mg/g [dry cell weight] to 22 ± 2.1 mg/g [dry cell weight]. The overexpression of truncated HMG1 in SM14, on the other hand, did not increase β-carotene production. The isoprenoid pathway is of a very complex phenotype and there are many direct and indirect variables involved in pathway performance. Even with these modifications to the hyper-producer strain, there seems to be limitations on β-carotene production. Further studies currently under investigation to increase β-carotene production include utilizing the fatty acid β-oxidation pathway for increasing the fatty acid content of the cell.

.

DEDICATION

To family and friends.

ACKNOWLEDGEMENTS

I would like to thank my committee chair, Dr. Katy Kao, and my committee members, Dr. Arul Jayaraman, Dr. Joshua Yuan, for their guidance and support throughout the course of this research.

Thanks also go to my friends and colleagues and the department faculty and staff for a great experience thus far at Texas A&M University. I also want to extend my gratitude to the National Education Foundation and the Texas Engineering Experimental Station, which provided financial support.

Finally, thanks to my family for their constant encouragement and support.

TABLE OF CONTENTS

	Page
ABSTRACT	ii
DEDICATION	iv
ACKNOWLEDGEMENTS	v
TABLE OF CONTENTS	vi
LIST OF FIGURES	viii
LIST OF TABLES	ix
1. INTRODUCTION	1
2. BACKGROUND AND LITERATURE REVIEW	5
2.1 Isoprenoid biosynthesis pathway	5
2.2 Oxidative stress response in yeast	7
2.3 The role of carotenoids	11
2.4 Metabolic engineering of *S. cerevisiae*	16
3. MATERIALS AND METHODS	21
3.1 Materials	21
3.2 Methods	23
4. RESULTS	30
4.1 Impact of bioreactor parameters on carotenoid production	30
4.2 Metabolic engineering of *S. cerevisiae*	35
5. DISCUSSION	37
6. CONCLUSIONS	40
REFERENCES	41

APPENDIX 52

LIST OF FIGURES

FIGURE		Page
1	Biosynthesis of isoprenoids by the mevalonate pathway	6
2	Cellular responses to oxidative stress in *Saccharomyces cerevisiae*	9
3	Carotenoid biosynthesis pathway	12
4	Various aspects of metabolic engineering	18
5	Mevalonate pathway in yeast and the carotenoid biosynthesis pathway of *X. dendrorhous*	19
6	Effect of aeration on SM14 carotenoid titer in correlation with pH	31
7	Effect of aeration on SM14 carotenoid production with respect to growth medium and pH	32
8	Maximum β-carotene produced in batch bioreactor	33
9	Carotenoid titer, biomass, and metabolite comparison of YNB batch run of SM14 and YLH2 (ancestral strain)	34
10	β-carotene quantification comparison between strains with tHMG1 and CTT1	36

LIST OF TABLES

TABLE		Page
1	Chemicals	22
2	Organisms	24
3	Plasmids	27
4	Oligonucleotides	28

1. INTRODUCTION

The synthesis of natural compounds by microbial systems is an emerging field in metabolic engineering for the application towards industrial biotechnology and production. There are many advantages of microbial-based compound production over the chemical synthesis or extraction of compounds including lower toxic waste production, carbon dioxide emissions, and energy requirements, as well as simpler purification processes, the potential for use of renewable feed stocks such as corn or soybeans, and the ability of enzymes to perform chiral synthesis on molecules [1]. Many natural products, such as active pharmaceutical ingredients (APIs), are not feasible for chemical synthesis due to structural complexities and are only able to be produced through a cellular means. These compounds have a high market value such that there is a desire to produce them in a heterologous host and reap the benefits. Pharmaceutical compounds may be the most valuable and have the highest profit margins, but fine chemicals and molecules such as vitamins, fragrances, and organic acids are also capable of being biologically synthesized. Currently, many precursors for known APIs and fine chemicals are successfully being engineered into microbe hosts, which is the next step towards tailoring the cell to produce specific compounds [2]. The different types of molecules and compounds that can be created through metabolic engineering are only beginning to be discovered and there is a potential for break-through product formations. Engineered microbial catalysts are becoming the new generation method for a sustainable and economical route to produce desired compounds.

Microbial systems that have been explored as heterologous production hosts include *Escherichia coli* and yeast [3-10]. The budding yeast *Saccharomyces cerevisiae* is the key model eukaryotic organism used extensively for metabolic engineering due to its well-studied genome and wide range of tools available for genetic modifications [1]. These two aspects make *S. cerevisiae* a great candidate as a biocatalyst for microbial production of natural products. *S. cerevisiae* is also favored for industrial processes due

to several factors such as its inherent robustness to high osmotic pressure and low pH, both of which are frequently encountered during industrial fermentation [2]. Yeast is also an economical organism to use because it grows quickly and at a low startup cost, which allows for high production throughput and quick turnaround time between batches.

So far, metabolic engineering has converted this microbe into a potential "cell factory" for production of a diverse range of chemical compounds [11]. There is continuous work being done to genetically control yeast to "debottleneck" the desired pathways and maximize desired product titer, yield, and productivity [2]. Isoprenoids, for example, are a class of compounds with the potential for microbial-based production. Isoprenoids are a diverse group of over 30,000 identified compounds in nature [12-14]. They are essential for proper cellular function, but they also have industrial value as pharmaceuticals (e.g. taxol, artemisinin), pesticides, and nutriceuticals (e.g. carotenoids) [15]. The majority of isoprenoid compounds are components of essential oils that occur naturally in plants, but they also function as defensive agents against pathogens, reproductive hormones, mating pheromones, pigments, constituents of membranes, and components of signal transductions pathways [13]. There are two known pathways for isoprenoid biosynthesis in nature: the mevalonate-independent methyl erythritol 4-phosphate (MEP) pathway and the mevalonate (MVA) pathway. In the MEP pathway, pyruvate and glyceraldehyde-3-phosphate (G3P) are synthesized into 1-deoxy-D-xylulose-5-phosphate (DXP) that is then used to produce MEP. The MVA pathway, most common in eukaryotes and the one utilized in *S. cerevisiae*, uses acetyl-CoA as the precursor to produce isopentenyl diphosphate (IPP) for mevalonate production [16]. The MVA pathway provides a promising route for the production of various natural compounds biosynthesized from the pathway precursors isopentenyl diphosphate (IPP) and dimethylallyl pyrophosphate (DMAPP).

Our goal is to focus on the integration and implementation of metabolic engineering tools in order to improve the productivity of yeast for maximum isoprenoid production. Current approaches generally focus on optimizing gene expressions and enzyme activities for the biosynthetic genes; however, genes outside the direct biosynthetic pathway of the target compound may play a role in productivity. Indeed, prior studies have revealed the complex phenotype of isoprenoid biosynthesis in microorganisms. For example, in a pre-engineered *E. coli* strain, a combination of gene deletions in the genome increased lycopene production [17]. These genes were found by model-based and transposon-based approaches. Some of the genes found were outside of the direct isoprenoid biosynthesis pathway and they increased the supply of precursors and cofactors that are important in the lycopene biosynthesis pathway. Even with the gene deletions, the lycopene production was still below the predetermined stoichiometric maximum. This demonstrated that there are still unknown limiting kinetic and regulatory factors that are not accounted for in the stoichiometric model and that the isoprenoid pathway does not have a completely linear relationship [17].

Previously, our lab developed a novel directed evolution approach to optimize the isoprenoid pathway in *S. cerevisiae*. Increasing oxidative stress has been shown to increase β-carotene production in *S. cerevisiae* [18], so the hypothesis was that oxidative stress can be used as a driving force for directed evolution to enhance carotenoids production. We integrated a heterologous carotenoid gene cassette crt YB/I/E from the red yeast *Xanthophyllomyces dendrorhous* into *S. cerevisiae* and used adaptive evolution with hydrogen peroxide stress as the selective pressure to select for carotenoid hyper-producers. The cytosolic catalase gene CTT1 was deleted from the genome to allow for more efficient hydrogen peroxide shocking experiments because CTT1 mediates the oxidative stress response in yeast. We reached more than 12 mg/g dry cell weight [dcw] of β-carotene shortly after the start of the evolution experiments. This was a 100% improvement over the unevolved ancestral strain, which had a β-carotene production of 6 mg/g [dcw]. After the population evolution, single mutants were isolated from each

shock time point. Hyper-producers were selected on the basis of growth (normal colony size) and increased carotenoid production in comparison to the population levels. Mutant SM14 was one of the highest producers that produced approximately 300% more β-carotene (18 ± 1 mg/g [dcw]) over the ancestral strain (6 ± 1 mg/g [dcw]).

My work has two primary goals, both of which aim to further optimize carotenoid production in *S. cerevisiae*. First, I will optimize the bioreactor conditions for carotenoid productivity in the hyper-producing mutant strain SM14. My first goal is achieved with the following objectives: 1) determine the influence of pH, agitation, bioreactor batch run time, and medium on carotenoid production, and 2) perform bioreactor metabolite analysis for understanding the influence of growth kinetics and cell metabolite consumption on carotenoid production. Second, I will test the hypothesis that the β-carotene production in the evolved mutant SM14 is limited by fatty acid content of the cell. To achieve my second goal, I will pursue the following objectives: 1) use rational metabolic engineering to improve carotenoid production (we expect an increase in the ancestral unevolved strain, but limited improvements in the evolved mutant) and 2) metabolic engineering to increase the fatty acid content of the cell.

2. BACKGROUND AND LITERATURE REVIEW

2.1 Isoprenoid biosynthesis pathway

Isoprenoids, also called terpenoids, are the largest class of naturally occurring molecules. The biosynthesis pathway for isoprenoid compounds has been highly conserved throughout evolution [19]. Plants have maintained the eukaryotic mevalonic acid (MVA) pathway in the cytosol, while evolving the methylerythritol phosphate (MEP) pathway from the endosymbiotic plastid ancestor [14]. Being that they are some of the most ancient molecules ever identified, isoprenoids and their derivatives have substantial roles in many life forms that include regulators of gene expression, reproductive hormones, components of membranes, vitamins, and antimicrobial agents [13, 19].

The isoprenoid pathway in yeast begins with acetyl-CoA, which is the product of acetate metabolism. Acetyl-CoA is also responsible for initiating the TCA cycle and is a precursor to the synthesis of lipids, several amino acids, and histone acetylation [20]. Acetyl-CoA synthetase (ACS) catalyzes the reaction of acetate to acetyl-CoA. ACS-2 is considered the aerobic version of the enzyme and is not detected under anaerobic conditions. ACS-1 is induced under fermentation conditions. Acetyl Co-A is metabolized by ERG10 and ERG13 into HMG-CoA. HMG-CoA is converted to mevalonate via the NADPH-requiring enzyme HMG-CoA reductase (HMGR), which is the rate-limiting step of the pathway [21-23]. The initial synthesis for isoprenoid compounds starts from two basic five carbon units, isopentenyl pyrophosphate (IPP) and dimethylallyl pyrophosphate (DMAPP) [24]. These carbon units are isomers of each other and are the building blocks for any isoprenoid compounds. Both isomers are capable of being further metabolized into geranyl diphosphate (GPP), farnesyl diphosphate (FPP), and geranylgeranyl diphosphate (GGPP), as seen in Figure 1 [1]. Naturally occurring precursors then convert these compounds into monoterpenes, sesquiterpenes, and diterpenes, respectively.

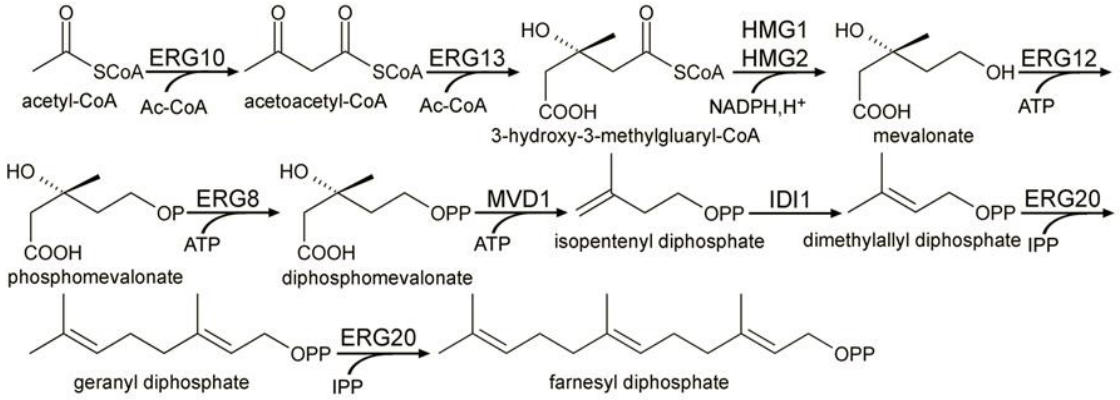

Figure 1. Biosynthesis of isoprenoids by the mevalonate pathway [1].

In the budding yeast *S. cerevisiae*, the isoprenoid pathway is responsible for the production of essential molecules such as prenylated proteins, polyprenyl alcohols, heme A, ubiquitone, and sterols. Prenylated proteins are proteins that have a farnesyl (C15) or geranylgeranyl (C20) isoprenoid covalently linked to the conserved cysteine residues or at the C-terminus of proteins [25]. Studies have shown that the Ras proteins, which are small G-proteins that play crucial roles in the signaling pathways controlling cell growth and differentiation, are farnesylated [25].The other isoprenoid geranylgeranyl is the predominant compound found on cellular proteins [25]. Polyprenyl alcohols are ubiquitous in minor components of membranes in yeast. They are synthesized from DMAPP and IPP and then used for protein N-glycosylation [26]. Ubiquitone (also known as coenzyme Q or CoQ) has ten isoprene units and is an isoprenylated benzoquinone. CoQ is a well-known component of the electron transport chain, and its main role is to transfer electrons from NADH dehydrogenase and succinate dehydrogenase to the CoQ:cytochrome c reductase in aerobic respiration and oxidative phosphorylation in the mitochondrial respiratory chain. CoQ also contributes significantly to ATP synthesis and acts as a lipid-soluble antioxidant in cellular membranes that scavenges for reactive oxygen species [27]. Ergosterol is an end product of the MVA pathway in *S. cerevisiae* and is the most prominent sterol in the

plasma membrane. Sterols are essential components of the plasma membrane in yeast and are used for intracellular endocytosis. Sterols are also important for protection against oxidative stress. Genome-wide expression analysis in yeast has identified a strong relationship of genes involved in ergosterol biosynthesis and oxidative stress protection [28]. Two areas in the cell with the highest concentration of sterols are the plasma membrane and secretory vesicles [29]. The cell would not be able to function properly without any of these products from the isoprenoid pathway.

2.2 Oxidative stress response in yeast

Yeast depends on oxygen for survival and aerobic respiration; however, they have had to evolve a multitude of defense systems to protect themselves from oxygen's toxic properties to the cell [30]. The extracellular environment of yeast is highly oxidative, providing for the need to maintain a reduced intracellular atmosphere. The reduced atmosphere is needed for proper protein formation and maintaining protein function [31]. Yeast cells generate a range of reactive oxidative species (ROS), which are usually the result of their aerobic metabolism but can also stem from environmental stress triggers [30, 32]. Known ROS that cause an inducible stress response are hydrogen peroxide, superoxide anion, and lipid peroxidation products [33]. Environmental stress triggers include the depletion of nutrients, increases in ambient temperature, or sudden xenobiotic contamination. Environmental changes invariably cause some stress on the cell, and this stress is frequently associated with ROS, which consume the antioxidants in the cell or further induce ROS accumulation [30].

Accumulation of ROS results in oxidative damage to crucial biomolecules such as proteins, DNA, and lipids. The accumulation of oxidized proteins has been associated with cellular aging and compromises cell viability. The result of protein oxidation is the formation of protein carbonyls, which can form large protein aggregates that cannot be degraded by proteolytic mechanisms. Non-degraded large protein aggregates eventually disrupt cell homeostasis completely [30]. ROS has the ability to cause mistranslation of

mRNA (for dysfunctional protein synthesis), and can also target the actin cytoskeleton of yeast (this results in accelerated aging and cell apoptosis). Oxidative DNA damage can result in base modification, abasic sites, protein-DNA cross linkage, and single or double stranded breaks in DNA. Oxidized DNA then interferes with the normal response to oxidative stress, which causes further ROS accumulation and programmed cell death (PCD). Lipid peroxidation is often the result of lipid oxidative damage and is initiated by the oxidation of polyunsaturated fatty acids (PUFAs) into lipid hydroperoxides, by $OH^{\bullet}$ radicals. *S. cerevisiae* produces saturated and monosaturated fatty acids of 16- and 18-carbon atoms and PUFAs of no more than two double bonds [34]. Most yeast are not capable of synthesizing long chain PUFAs, but will readily incorporate them into their membranes if cultured with PUFA rich medium. This further increases the risk of oxidative stress to the cell [30].

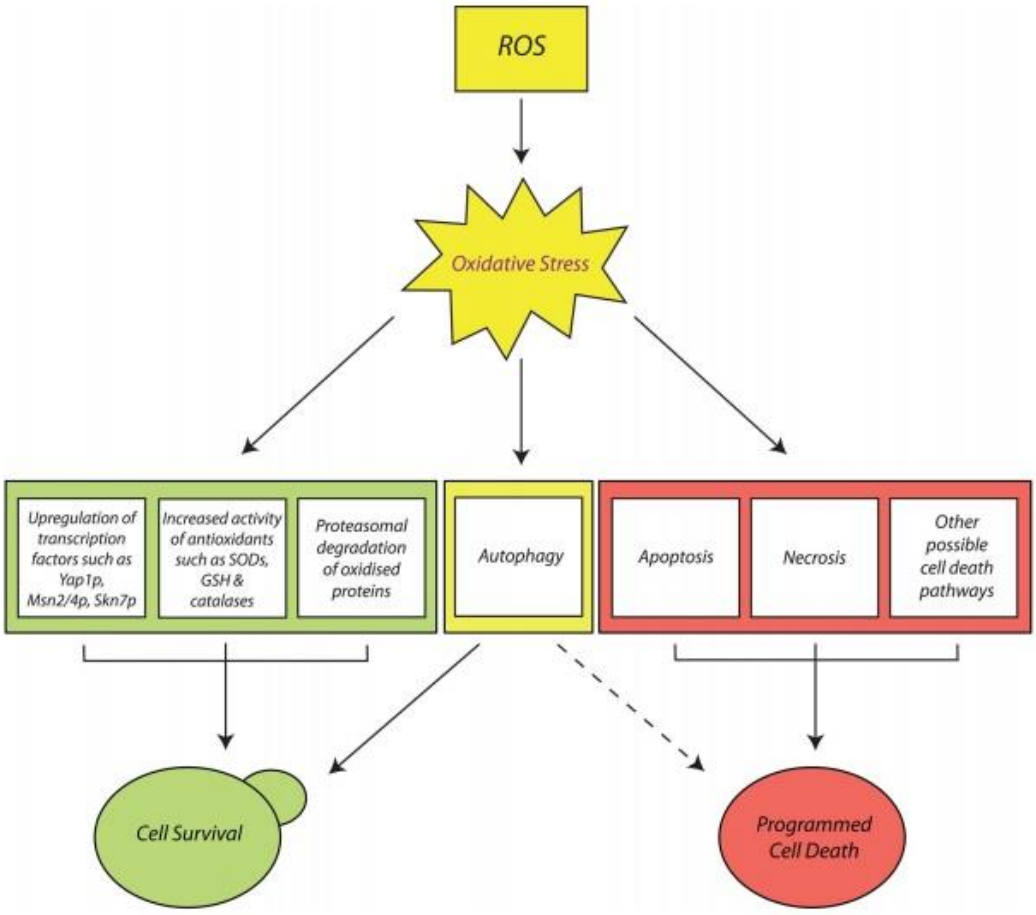

Figure 2. Cellular responses to oxidative stress in *Saccharomyces cerevisiae*. Oxidative stress can result in either cell survival (shown in green) or cell death (shown in red). ROS can activate enzymatic (catalases) and non-enzymatic antioxidants (such as GSH). These response systems work together with the targeted removal of small, oxidized proteins by the ubiquitin-dependent proteasome system (UPS) to keep cells alive. Cells can activate cytoprotective autophagic pathways (yellow) that remove irreparable oxidized macromolecules or dysfunctional organelles, such as mitochondria. An abnormally high degree of autophagy will result in programmed cell death (PCD). If the cell is exposed to severe oxidants, lethal response pathways such as apoptosis and necrosis will be activated [30].

There are both non-enzymatic and enzymatic stress responses in yeast, as seen in Figure 2 [30]. Non-enzymatic defense systems include but are not limited to the tripeptide glutathione (GSH), polyamides, lipid-soluble antioxidants, trehalose, metallothioneins, and glutaredoxin [33]. A study showed that glutathione deficient mutants are hypersensitive to H_2O_2 and also exhibit a slower growth rate and a longer lag phase than typical wild type cells. Glutathione has also been linked with protecting mitochondria from oxidants in the aerobic respiratory chain process [33]. Lipid soluble antioxidant molecules in yeast are also important for resistance to ROS. Cells with membranes containing higher amounts of saturated fatty acids are more resistant to oxidation effects than those cells with a higher concentration of PUFAs [33]. Autoxidation of PUFAs is a natural consequence of an oxygen rich environment and the lipid peroxidation products deteriorate membrane fluidity and cause oxidative damage to other biomolecules [35].

Enzymatic stress responses in yeast include catalase genes, pentose phosphate pathway enzymes, glutathione reductase and peroxidase, thioredoxin peroxidase and reductase, and the methionine reductase. The catalase genes CTA1 and CTT1 in *S. cerevisiae* play a role as peroxide scavengers and are responsible for the breakdown of H_2O_2 into O_2 and H_2O. H_2O_2 is a product of the fatty acid β-oxidation pathway and both catalase genes help in resistance towards H_2O_2 [33]. Cytosolic catalase T (CTT1) gene in *S. cerevisiae* has shown to be regulated by the supply of essential nutrients around the cell. Expression levels of CTT1 are low when grown in rich and complete media, but if any of the essential nutrients become limiting, expression levels rise substantially [36]. Overexpression of the CTT1 gene in *S. cerevisiae* has been shown to reduce overall ROS levels in the cell, which further helps maintain a normal amount of fatty acids in the cell [37]. The pentose phosphate metabolic pathway, which also aids in ROS protection in cells, produces nucleotides, antioxidants, and some lipids. The pathway includes glucose 6-phosphate dehydrogenase (ZWF1), transketolase (TKL1) and ribulose 5-phosphate epimerase (RPE1). All are involved in cellular reduction via the production of NADPH, which promotes more antioxidant presence that results in increased tolerance to H_2O_2

stress. Glutathione and thioredoxin are both powerful antioxidants. The glutathione reductase maintains a high ratio of reduced to oxidized components in the cell and glutathione peroxidase catalyzes the reduction of hydroperoxides via GSH as a reductant. Thioredoxin peroxidase works in conjunction with thioredoxin reductase to reduce both H_2O_2 and alpha hyperperoxides inside the cell [33].

2.3 The role of carotenoids

Carotenoids are naturally occurring terpenoid compounds of various pigments and serve many roles in microorganisms. They have the ability to protect cells against various ROS by catalytically quenching singlet oxygen species (O_2) that are generated from cellular metabolism. Carotenoids are present in both photosynthetic and non-photosynthetic organisms, where they carry very diverse functional roles. In nonphotosynthetic organisms, one of the main functions is to isolate toxic oxygen species from the environment [38]. Carotenoids also increase membrane rigidity to help reduce the penetration of singlet oxygen species from the extracellular environment [39].

Carotenoids consist of a polyene chain of conjugated bonds with varying amounts of isoprene units. They are responsible for the different pigmentations seen in nature that absorb at a wavelength from 300 to 600 nm. The absorbance of the molecule is correlated to the number of conjugated bonds and functional groups. Two broad classifications of carotenoids include hydrocarbons (carotenes) and oxygenated derivatives (xanthophylls). Phytoene ($C_{40}H_{56}$) is a symmetrical acyclic C40 hydrocarbon structure that is formed by the condensation of two geranylgeranyl diphosphate (GGPP) molecules. It is the initial "colorless" carotenoid from which other carotenoid compounds are derived via various biochemical reactions. This group consists of about 600 natural carotenoids and are mostly formed by enzyme mediated reactions [38]. Important carotenoids produced from microorganisms include β-Carotene, α-Carotene, β-Cryptoxanthin, Lutein, Zeaxanthin, Astaxanthin, Canthaxanthin, Neoxanthin, Violaxanthin, Antheraxanthin, and Fucoxanthin, as seen in Figure 3 [39].

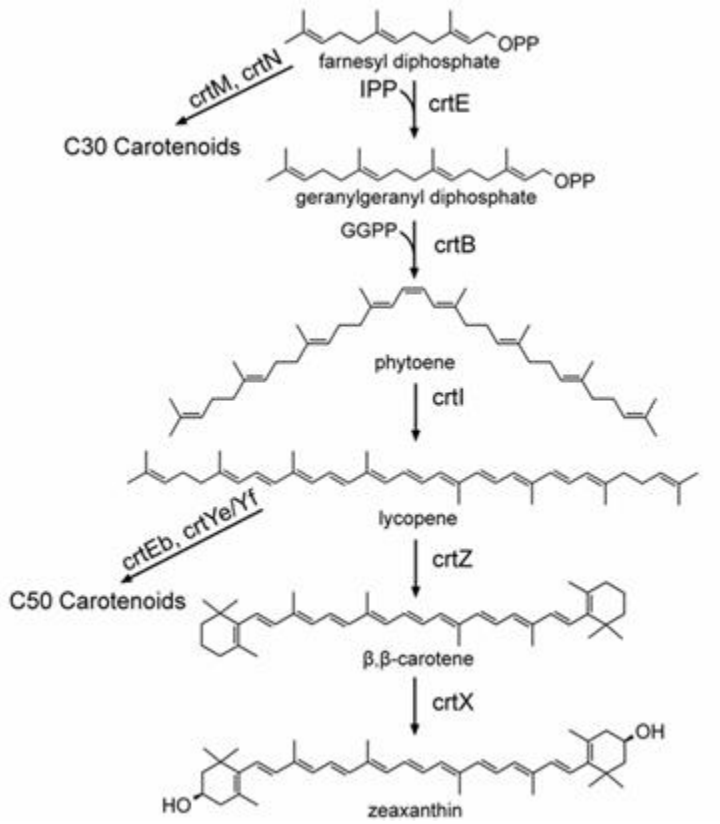

Figure 3. Carotenoid biosynthesis pathway [1].

The evolutionary origins of carotenoids are thought to be from ancient anoxygenic photosynthetic microorganisms, long before the time of eukaryotes. The phylum of bacteria known as cyanobacteria is the earliest record of oxygenic carotenoid producing bacteria that dates back 3.5 billion years with fossil and molecular evidence. Through microbe evolution, the carotenoid biosynthetic pathways diversified, which resulted in different structural forms of carotenoid molecules. The earths transition from an anaerobic to aerobic environment also impacted carotenoid diversity and their dependence on oxygen-dependent enzymes [39]. Carotenoids are believed to have evolved similar to sterols, which evolved in parallel to the appearance of atmospheric oxygen [38]. Eukaryotes then acquired the mechanism for carotenoid production either

by symbiotic growth with bacteria or via eukaryotic chloroplasts [38]. Prochlorophytes, which is another group of oxygenic photosynthetic bacteria, have similarities in carotenoid pigments to that of algae and eukaryotic plants. This also suggests crossover of evolutionary relations between species [39].

Carotenoids form a unique medicinal and biotechnological class of natural pigments. They are structurally very diverse and are involved in many biological functions such as species coloration, photo protection, light harvesting, and are precursors to many hormones. Commercially, carotenoids are used in pharmaceuticals, cosmetics, food colorants, and in animal feed supplements [40]. The health benefits of carotenoids are becoming increasingly more understood. Carotenoids are not synthesized in animals, but act as pro-vitamin A compounds and can be metabolized into vitamin A and retinoids as a nutrition source. Studies have shown that carotenoid compounds also exhibit disease-fighting power and are able to prevent or slow down the presence of cancer or other chronic diseases such as multiple sclerosis, cataracts and arteriosclerosis [38].

The market for carotenoid supplements is large and constantly growing. As of 2010, commercially used carotenoids had a value at nearly $1.2 billion with a projected value of $1.4 billion by 2018. Of that total value, β-carotene had a market value of $261 million in 2010, which is roughly 20 percent of the total carotenoid value [41]. The majority of carotenoids on the global market are chemically synthesized or extracted via solvents from non-microbial sources [39]. In lieu of non-organic means of obtaining carotenoids, there are few viable options for microbe-based carotenoids that give competition to the chemically synthesized molecules. There is a growing consumer preference for natural additive supplements and an economical preference for production of carotenoids in microbes because of a potentially lower production cost [39]. Currently, the most commonly used microbes for natural carotenoid synthesis are *Dunaliella salina* for β-carotene and *Haematococcus pluvialis* or *X. dendrorhous* for

astaxanthin [42]. Further research is still needed to develop more technologies and to metabolically engineer other organisms to produce carotenoids.

In general, factors affecting carotenoid production in microorganisms include light, temperature, chemical compounds, metals ions and salts, and solvents [42]. In the organism *X. dendrorhous*, astaxanthin production is proposed to be photo-inducible because an increase of carotenoid production is observed when exposed to strong light illumination. Reactive oxygen species are also seen as active participants and linked to improvements in carotenoid production [18, 42]. Temperature influences the growth and development of living organisms. It has the potential to alter the activity and concentrations of the enzymes involved in biosynthetic pathways, which reflects the activity of the isoprenoid production pathways. Across microorganisms, a lower temperature generally promotes a higher rate of carotenoid production. The hypothesis behind this phenomenon is that as temperature decreases, the membrane fluidity and functionality also decrease. This decrease in fitness is then compensated in the cell by overproduction of carotenoids and unsaturated lipids [42].

To further understand the carotenogenic biosynthesis pathway in various organisms, researchers have explored chemical compounds and their impact on the pathway. For example, in the fungi species *Blakeslea trispora*, when penicillin (1 mg/L) was added to the culture after 24 hours of growth, carotenogenesis was stimulated by 50 percent without disrupting the total protein and carbohydrate synthesis. Authors suggested that penicillin stimulates the early stages of the isoprenoid pathway because mevalonate kinase was close to double in concentration under the presence of penicillin [42]. Similarly in *Rhodotorula mucilaginosa*, which is a unicellular pigmented yeast, chloramphenicol (1,000 mg/L) had a positive effect on total carotenoid production [42]. The yeast genus *Rhodotorula* also demonstrated an improvement of carotenoid volumetric production (mg/L) and yield when exposed to calcium, copper, zinc, and ferrous ions in the growth medium. The explained rationale behind this behavior is that

there is either a stimulation of carotenoid-synthesizing enzymes from the cations or that there is an increase in active oxygen free radicals in the surrounding medium [42].

Solvents in the extracellular environment may also affect carotenoid production in microorganisms. The addition of ethanol, methanol, isopropanol, and ethylene glycol to the culture medium has been shown to help increase carotenoid production in microbes. When 2% (v/v) ethanol was added to the culture of *Rhodotorula*, there was a reported increase in β-carotene and a decrease in torulene. Torulene is a hydrocarbon carotenoid compound with only one cyclic end (versus two cyclic ends in β-carotene) [43]. It has been proposed that there is ethanol-mediated inhibition of torulene oxidation, which suggests that the there is a metabolic pathway shift to favor ring closure (as seen in β-carotene). There was also a similar phenomenon seen in the red yeast *X. dendrorhous* (*Phaffia rhodozyma*) when 0.2% (v/v) ethanol was added to the culture medium [43]. Further detailed studies then indicated that ethanol activates oxidative metabolism with the induction of HMG-CoA reductase. HMG-CoA reductase is a key enzyme in the isoprenoid biosynthesis pathway. The activation of this enzyme naturally results in enhanced carotenoid production [43].

The study of the natural red yeast *X. dendrorhous* has provided more knowledge about the factors affecting carotenoid yield. Additives to culture medium such as ethanol, acetate, and mevalonate have all resulted in an increase of carotenoid formation; however, any supplement such as mevalonate is not economically feasible for long-term industrial production. When *X. dendrorhous* is grown with additional ethanol, carotenoid production was continuously enhanced as ethanol was added and the effect of ethanol was greatest at 3 and 5 days. From this result, it is assumed that ethanol increases the carotenoid production once cells are in the stationary phase [43]. A decrease in pH is also observed in *X. dendrorhous* cultures when they are grown with added ethanol. This pH drop is possibly the result of acetate accumulation in the culture, but regardless the carotenoid levels increase [43].

2.4 Metabolic engineering of *S. cerevisiae*

The baker's yeast *Saccharomyces cerevisiae* is a model organism for genetic and metabolic engineering. It is a Generally Recognized As a Safe (GRAS) organism, has a short life cycle, and is easy to culture [9].The genome is highly malleable and is responsive to rearrangements and manipulations by recombinant DNA technology, which is even further expedited by the availability of the complete genome sequence of *S. cerevisiae* published in 1996 [44]. It is a fairly robust and genetically stable host that is capable of production of fine and bulk chemicals with proper engineering [2, 9]. Strains are also being engineered for increased tolerance to ethanol and other end products, which makes *S. cerevisiae* more conducible to large scale fermentation [45].

Development of more sophisticated methods in the field of recombinant DNA technology has enabled researchers to manipulate a given pathway of interest. This manipulation is a more direct approach for cell improvement and involves introducing specific genome perturbations such as modifying promoter strength of a gene, gene deletions, or establishing new genes and/or new metabolic pathways into the cell [44]. Metabolic engineering is a directed approach, which distinguishes it from classical applied molecular biology. Metabolic engineering generally includes two aspects. The first aspect is the analytical side, which involves analysis of the cells to identify the most promising targets for genetic manipulation. The second aspect is the genetic engineering of the cell that encompasses the actual construction of the genetic modifications into the cell [44]. Different targets for metabolic engineering in *S. cerevisiae* are as follows: improvements of productivity and yield, elimination of by-products, improvements of cellular properties and process performance, extension of substrate range, and extension of product range including heterologous protein production [44].

The molecular toolset for transforming *S. cerevisiae* is constantly expanding. Over the past several decades, technologies have rapidly evolved enabling yeast to produce a broad range of molecules by synthetically altering the genome [46]. A large majority of

these systems involve plasmid DNA and vectors with tunable parameters such as promotor/terminator, selection markers, and CEN/ARS origins of replication [47]. The transformation of yeast with these unique plasmids often comes at a metabolic cost to the cell, which may include a decreased growth rate or a decrease in production of the desired products [48]. The choice of selection marker, for example, has varying side effects to the cellular metabolic burden. Auxotrophic markers (out of the various selectable markers available) dramatically changed the specific growth rate of the strain and the most significant plasmid load was found to be in a diploid *S. cerevisiae* yeast strain [47]. The same study showed that plasmid copy number is not always determined by the origin of replication. They demonstrated that the use of the dominant antibiotic marker KanMX completely masks the effects of different origins of replication but surprisingly does not affect the specific growth rate of the strain [47]. Research has also shown that introduction of centromeric plasmids may result in higher heterologous protein expression, which may cause a negative gene dosing effect on the cell [47, 49]. Indeed, there seems to be a large disconnect between the use of plasmid-borne systems and integrated DNA cassettes that should be taken into consideration when utilizing metabolic engineering for product formation in yeast.

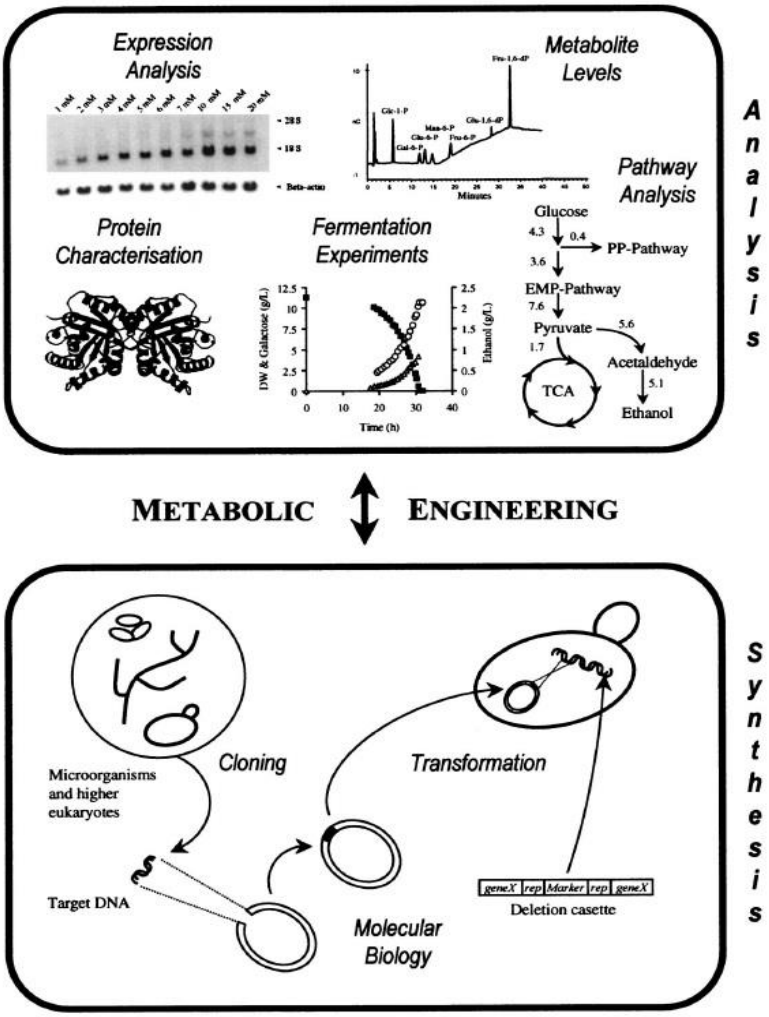

Figure 4. Various aspects of metabolic engineering [44].

Metabolic engineering is rarely a straightforward process. Cellular metabolism, for example, has a high level of complexity in *S. cerevisiae* and is a limiting factor for analytical methods of metabolic engineering. The two aspects of metabolic engineering (as seen in Figure 4) are both crucial in order to fully understand the interactions between enzyme concentrations, metabolite levels, and gene expression [44]. The isoprenoid production pathway in *Saccharomyces* is affected by a multitude of direct and indirect factors including the overexpression of HMG-CoA, the effect of ethanol on HMG-CoA activity, and yeast growth substrates. The regulation of HMGR has been the

main focus for isoprenoid biosynthesis ever since it has been shown to be the rate-limiting step in the pathway [21-23]. This natural bottleneck observed in the pathway has been a target for overexpression in *S. cerevisiae* to increase mevalonate pathway product yields [10]. This approach has been shown to moderately increase the flux towards the mevalonate pathway for isoprenoid production such as carotenoids and non-isoprenoid compounds like bisabolene (as seen in Figure 5), a precursor to biofuel bisabolane [10, 50].

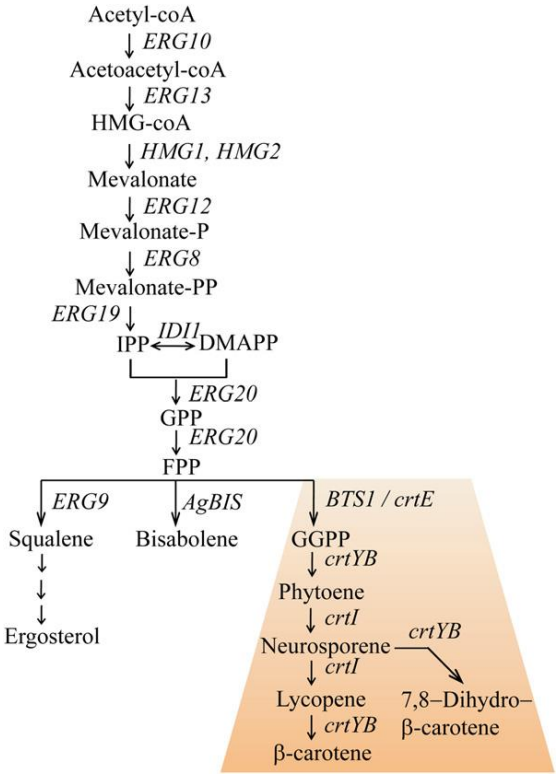

Figure 5. Mevalonate pathway in yeast and the carotenoid biosynthesis pathway in *X. dendrorhous* [15].

Both *E. coli* [3] and *S. cerevisiae* [43] have been studied to understand the impact of overexpressing the isoprenoid biosynthesis pathway. *E. coli* has physical limitations for

accumulation of carotenoids in the cell membrane that is most likely already reached without any modifications to the cell storage capabilities. Yeast, on the other hand, are capable of storing large amounts of ergosterol inside of the cell [51]. The ergosterol pathway has been diverted for carotenoid production in noncarotenogenic species such as *S. cerevisiae* and *Candida utilis*. The knowledge of a number of carotenoid biosynthetic pathways has also provided for a unique toolbox of carotenogenic (crt) genes that can be used for carotenoid production in *S. cerevisiae* via strain engineering of the terpenoid biosynthesis pathway [51]. The strains have been successfully engineered to produce carotenoids and optimized through overexpressing the bottleneck HMG1 and deleting ERG9. The ERG9 gene encodes for squalene synthase, and deleting it disrupts the ergosterol biosynthesis pathway, thus increasing the flux towards carotenoid production [51].

Carotenoids are intracellular components and are not naturally secreted outside of the cell during fermentation [45]. The most effective ways to increase β-carotene production involves either increasing the biomass production or to increase the efficiency of the carotenoid production pathway. Carotenoid synthesis is governed by the activity of the isoprenoid pathway enzymes [45]. Balancing enzyme expression and relative expression levels are still crucial to the stability of the cell and its natural metabolic functions [2]. Altering the copy number of the gene is a standard approach for increasing metabolic flux; however, changing the promotor strength, ribosomal binding strength, and stability of the mRNA and resulting proteins are all variables to test in the optimization process [2].

3. MATERIALS AND METHODS

3.1 Materials

3.1.1 Medium

All medium was autoclaved at 121ºC. Heat sensitive antibiotics were sterile filtered and added to cooled media (56 ºC). For all agar plates, final agar concentration is 2% (wt/vol). *Escherichia coli* medium included Luria-Bertani broth (18 g/L tryptone broth, 5 g/L yeast extract, 2 g/L NaCl) and Super Optimum (SOC) broth (20 g/L tryptone, 5 g/L yeast extract, 0.5 g/L NaCl, 2.5 mL/L 1M KCl, 10 mL/L 1M $MgCl_2$, 10 mL/L 1M $MgSO_4$, 20 mL/L 1M dextrose). 100 µg/mL Ampicillin (100 mg/mL) was used for selection purposes. *S. cerevisiae* medium included YPD medium (10 g/L yeast extract, 20 g/L peptone, 20 g/L dextrose), YNB medium (1.7 g/L yeast nitrogen base without amino acids and ammonium sulfate, 20 g/L dextrose, 5 g/L ammonium sulfate). 300 µg/mL of Hygromycin B (100 mg/mL, H_2O) and 100 µg/mL Nourseothricin (100 mg/mL, H_2O) were used for selection. Buffer and solutions included LiAc/TE (100 mM LiAc, 1X TE pH 7.5), SS DNA/PEG/TE/LiAc (0.26 µg/µL salmon sperm DNA, 0.4 g/L PEG 3350, 1X TE pH 7.5, 100 mM LiAc), TE (100 mM Tris-Cl, 10 mM EDTA). All chemicals used in this work may be seen in Table 1.

Table 1. Chemicals

Manufacturer	Location	Chemicals
ACROS	USA	D(+)-glucose, agar
Amresco	USA	Peptone, Yeast Nitrogen Base
BDH Aristar	USA	HCl, Ammonium Sulfate
Electron Microscopy Science	USA	PEG 3350
EMD Chemicals Inc.	Germany	Yeast Extract
Enzo Life Sciences	USA	Hygromycin B
Fisher Scientific	USA	EDTA
Jena Biosciences	Germany	Nourseothricin
JT Baker	USA	Antifoam B Silicone Emulsion, NaCl
MP Biosciences	USA	LiAc
Promega	USA	Tris-Cl
Teknova	USA	NaOH, Tryptone Broth
Tokyo Chemical Industry Co., LTD	Japan	Dodecane
Trevigen Inc.	USA	Salmon Sperm DNA

3.2 Methods

3.2.1 Cultivation and storage of *E. coli*

The *E. coli* strain BW25113 (Table 2) was used for all plasmid constructions and cultivated in Luria-Bertani medium at 37ºC at 225 rpm. For selection and cultivation of transformants, LB agar plates and LB medium were supplemented with 100 µg/mL ampicillin. For long term storage, frozen stocks were made of each transformant by suspending cells in a ~17% glycerol solution followed by storage in cryogenic tubes at -80 ºC.

3.2.2 Transformation of *E. coli* by electroporation

The *E. coli* strain BW25113 was grown overnight at 37ºC in a 3 ml culture of LB medium. After 12 hours, 500 µL of the culture was back diluted into 50 mL of fresh LB medium. The diluted cells were incubated at 37ºC until they reached an OD600 of 0.4. The cells were harvested by centrifugation at 5000 rpm, washed twice with 20 mL ice cold sterile milliQ water, once with 10 mL ice cold sterile 10 % glycerol solution. After the final wash step, cells were resuspended in ~500 µL of 10% glycerol and added into sterile microcentrifuge tubes in 50 µL aliquots. Any extra aliquots were stored in the -80 ºC freezer. For electroporation, 2 µL of cleaned DNA was added to 50 µL of competent cells and allowed to sit on ice for 5 minutes. The mixture was pipetted into a sterile cuvette and contents were electroporated at 25 µF, 200 ohms, and 1800 V. 1 mL of SOC recovery medium was added to the cuvette and cells were incubated at 37ºC for one hour.

3.2.3 Cultivation and storage of *S. cerevisiae*

All yeast strains were grown at 30ºC in solid or liquid YPD growth medium with 2% D-glucose. For selection of hygromycin B resistant transformants, YNB agar plates supplemented with 300 µg/mL of hygromycin B were used. For selection of nourseothricin resistant transformants, YNB agar plates supplemented with 100 µg/mL of nourseothricin were used. Yeast were plated on YPD agar plates at room temperature

for short term storage. All yeast strains used in this work may be seen in Table 2. For long term storage, frozen stocks were made of each transformant by suspending cells in a ~17% glycerol solution followed by storage in cryogenic tubes at -80 ºC.

Table 2. Organisms

Organism	Strain	Genotype	Reference
E. coli	BW25113	rrnB3 ΔlacZ4787 hsdR514 Δ(araBAD)567 Δ(rhaBAD)568 rph-1	Barry Wanner
S. cerevisiae	FY2 (GSY1136)	Matα, ura3-52, gal+ in S288c background, YBR209W::Act1p-GFP-Act1t-URA3	Kao and Sherlock (2008) [52]
	YLH1	GSY1136::YIplac211YB/I/E	Reyes et al. (2014) [53]
	YLH2	GSY1136::YIplac211YB/I/E ΔCTT1	Reyes et al. (2014) [53]
	SM14	YLH2 mutant P1A2. Isolated hyper-producer from evolution experiment.	Reyes et al. (2014) [53]
	YMO1	SM14::CTT1	This work
	YMO3	YLH2::CTT1	This work
	YMO2	SM14::CTT1, pAG36::TDH3p-tHMG1-ACTp	This work
	YMO4	YLH2::CTT1, pAG36::TDH3p-tHMG1-ACTp	This work

3.2.4 Transformation of *S. cerevisiae* by heat shock

A modified lithium-acetate method was used for heat shock transformations [54, 55]. Cells were grown overnight at 30ºC in 3 mL of YPD medium. After 12 hours, roughly 500 µL of overnight culture was added to 50 mL of YPD medium for an OD600 of 0.05. Diluted cells were incubated at 30ºC for 4-5 hours until the OD600 was 0.6. Cells were harvested by centrifugation, washed twice with 30 mL sterile water, once with 10 mL LiAc/TE, resuspended in 100 µL of LiAc/TE, and incubated at 30ºC for 30 minutes without agitation. To a sterile microcentrifuge tube, components were added in the following order: 20 µL DNA, 10 µL of 10 mg/mL single stranded salmon sperm DNA, 300 µL of PEG/LiAc/TE, 50 µL of competent cells. Tubes were gently inverted to mix and incubated at 30ºC for 30 minutes without agitation. Cells were then heat-shocked for 20 minutes at 42ºC, pelleted, and resuspended in 1 mL of YPD medium. After one hour, cells were washed and resuspended with 1 mL of sterile water. 100 µL of culture was plated on selective plates and plates were incubated at 30ºC for 2-3 days.

3.2.5 Construction of CTT1 integration plasmid

Plasmid pAG26 with hygromycin B selection (Table 3) was used as the backbone vector for construction of the CTT1 integration plasmid. The CTT1 sequence was amplified from genomic DNA of wild type FY2 *S. cerevisiae* using primers F-CTT1-HindIII and R-CTT1-SalI, digested with HindIII and SalI and ligated into pAG26 cut with the same enzymes. The downstream portion of CTT1 for marker recycling purposes was amplified using primers F-DSCTT1-ClaI and R-DSCTT1-SpeI (Table 4), digested with ClaI and SpeI and ligated into pAG26 cut with the same enzymes. Once constructed, the plasmid was electroporated into *E. coli* strain BW25113 and plated on LB agar plates supplemented with 100 µg/mL of ampicillin. The plasmid was digested with StuI and PvuII prior to transformation to ensure proper integration at the CTT1 gene site. Transformation colonies were selected and grown in 3 ml LB with 100 µg/mL ampicillin. A frozen stock was saved for long term storage and plasmid extractions were

verified using PCR. Once confirmed of having the right construct, plasmids were transformed into yeast strains using the lithium-acetate method [54, 55].

3.2.6 Construction of truncated HMG1 overexpression plasmid

The truncated HMG1 gene involved in the mevalonate pathway was PCR amplified from genomic DNA of wild type FY2 *S. cerevisiae* using Accura^{TM} High Fidelity DNA Polymerase. The overexpression plasmid was constructed by first digesting the yEpGAP-cherry plasmid (containing the TDH3 promotor) with EcoRI and XhoI, and gel extracting the plasmid without the yeast enhanced monomeric red fluorescent protein (yEmRFP). The tHMG1 PCR was digested with EcoRI and XhoI and ligated into the backbone vector of yEpGAP. The ligation product was transformed into BW25113 *E. coli* and selected on LB plates with 100 μg/ml ampicillin. Transformants were verified via colony PCR. Primers F-ACTt-XhoI and R-ACTt-SalI were used to amplify the ACT terminator sequence from plasmid pKKGS4 (Table 3 and 4). The PCR amplified ACT terminator and the yEpGAP::tHMG1 plasmid were digested with XhoI and SalI and ligated at room temperature for 2 hours. The ligated plasmid was transformed and propagated into BW25113 *E. coli* in LB with ampicillin. The TDH3p:tHMG1:ACTt construct was cut from the yEpGAP plasmid using restriction enzyme BamHI and ligated into pAG36 with nourseothricin resistance. The ligated plasmid was transformed and propagated into BW25113 *E. coli* under ampicillin selection, and further transformed into yeast using the lithium-acetate method [54].

Table 3. Plasmids

Name	Marker	Description	Reference
yEpGAP-cherry	Amp, RFP	Source for TDH3 promoter	Neta Dean
pKKGS4	Amp	Source for ACT terminator	Katy Kao
pAG26 (Addgene 35127)	Amp/hph/URA3	CEN plasmid with Hygromycin B selection	John McCusker [56]
pAG36 (Addgene 35126)	Amp/NAT/URA3	CEN plasmid with Nourseothricin selection	John McCusker [56]

Table 4. Oligonucleotides

Name	Sequence	Description
F-CTT1-HindIII	5'-TGAGAAGCTTGAGC TGCTAAACATTAA-3'	Forward primer to amplify CTT1 gene from FY2
R-CTT1-SalI	5'-TGAGGTCGACTTAA TTGGCACTTGC-3'	Reverse primer to amplify CTT1 gene from FY2
F-DSCTT1-ClaI	5'-TGAGATCGATGGCA GCACTATTTATT-3'	Forward primer to amplify downstream of CTT1 gene from FY2
R-DSCTT1-SpeI	5'- TGAGACTAGTGAGA TAGGTGGAATCTTA -3'	Reverse primer to amplify downstream of CTT1 gene from FY2
F-tHMG1-EcoRI	5'-TGAGGAATTCATGG ACCAATTGGTGAAAA-3'	Forward primer to amplify tHMG1 from FY2
R-tHMG1-XhoI	5'-TGAGCTCGAGTTAG GATTTAATGCAGG-3'	Reverse primer to amplify tHMG1 from FY2
F-ACTt-XhoI	5'-TGAGCTCGAGCAAA TAGGCGGC-3'	Forward primer to amplify ACTt from pKKGS4
R-ACTt-SalI	5'-TGAGGTCGACTTAC GCGCTTTTCC-3'	Reverse primer to amplify ACTt from pKKGS4

3.2.7 Quantitative characterization of carotenoid levels

Quantification of carotenoids was done as described previously with the following modifications [53]. 500 μL of cell culture was transferred to a 2 mL collection tube and cells were collected via centrifugation at 12,000 rpm for 2 minutes. Supernatant was aspirated and the pelleted cells were disrupted in 1 mL of dodecane and approximately 250 μL of 425-600 μm acid-washed glass beads (Sigma). Disrupted culture was centrifuged for 2 minutes at 12,000 rpm and 200 μL of the supernatant was transferred to a Corning® 96 well black-wall clear-bottom plate for further quantification.

3.2.8 Bioreactor studies

Both YPD and YNB media supplemented with 2% (wt/vol) D-glucose were used for bioreactor studies. The seed cultures for fermentation were started using a 1 mL frozen culture stock (thawed) into 50 mL of media. Frozen culture starter stocks were created from an initial YPD batch-mode bioreactor run, which were then used to inoculate 50 mL baffled flasks. Seed cultures were grown for 48 hours at 30°C and 170 rpm. The 50 mL culture was used to inoculate 3 L of media in a 7 L bioreactor. Bioreactor studies were conducted in a 7 L glass bioreactor (Applikon®) for 72 hours. Bioreactor pH was maintained at set point using 2 M NaOH and 2 M HCl. The temperature was maintained at 30°C with an agitation speed of 800 rpm and continuous air flow.

4. RESULTS

4.1 Impact of bioreactor parameters on carotenoid production

β-carotene production and the metabolic profiles of each batch run varied based on media composition, agitation speed, and pH. Bioreactor runs were conducted with either YPD or YNB media and at an agitation speed of 400 or 800 rpm. The pH levels tested were 4, 4.5, and 5. YPD is a complete media, which results in a high titer (mg β-carotene/L) and biomass (g/L); however, it also results in performance variability due to the yeast extract in the culture medium. Conversely, YNB is a defined media that allows for reproducibility and higher β-carotene production (mg β-carotene/g [dcw]) at the exchange of a lower final biomass. Another variable is agitation speed, which affects the amounts of aeration and dissolved oxygen (DO) levels in the bioreactor.

Carotenogenesis is an aerobic process [57], so the agitation speed influences both carotenoid production and metabolite concentrations. The maximum observed drop in DO for each run happens during the exponential growth phase when cells are consuming the most oxygen. The maximum DO drop for runs at 400 rpm is 80-90% and only 40-50% for runs at 800 rpm. At 800 rpm, the β-carotene production follows a linear trend throughout the run. When the agitation speed is lower, there is an evident lag time in β-carotene production, as shown in Figure 6. This lag time is most likely the result of limiting oxygen in the bioreactor. Despite the different production profiles, the final amounts of β-carotene produced are similar between the two agitation speeds. Aeration level also affects the ethanol consumption rate in the bioreactor. For most runs at 800 rpm, ethanol is consumed within 24 hours; however, ethanol takes about twice as long to be consumed when agitation is at 400 rpm.

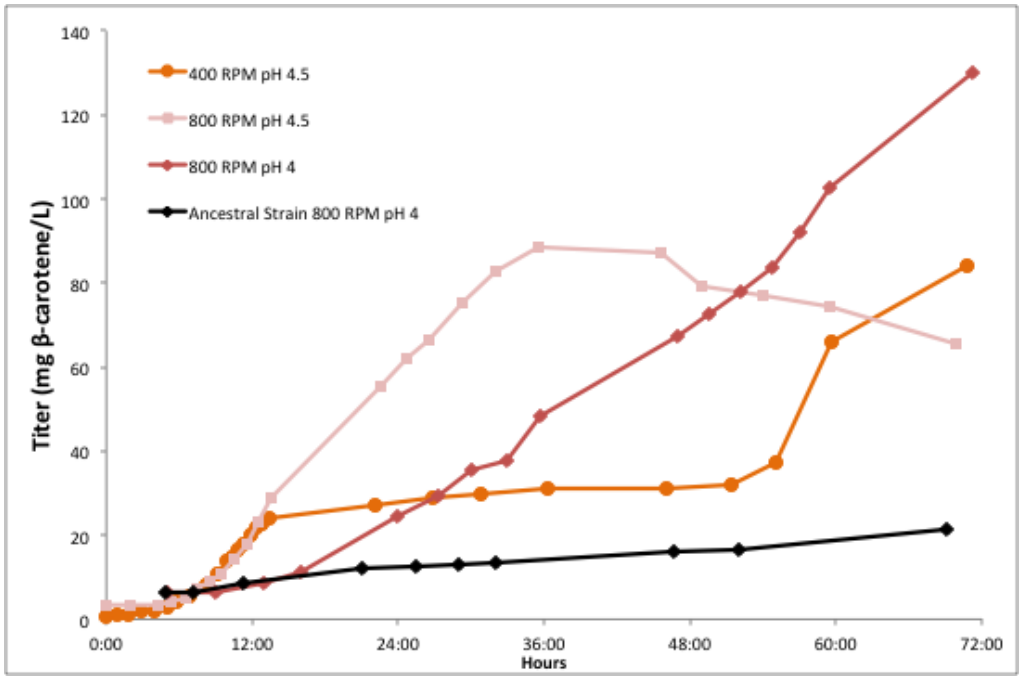

Figure 6. Effect of aeration on SM14 carotenoid titer in correlation with pH. YNB medium, varying agitation speed and pH.

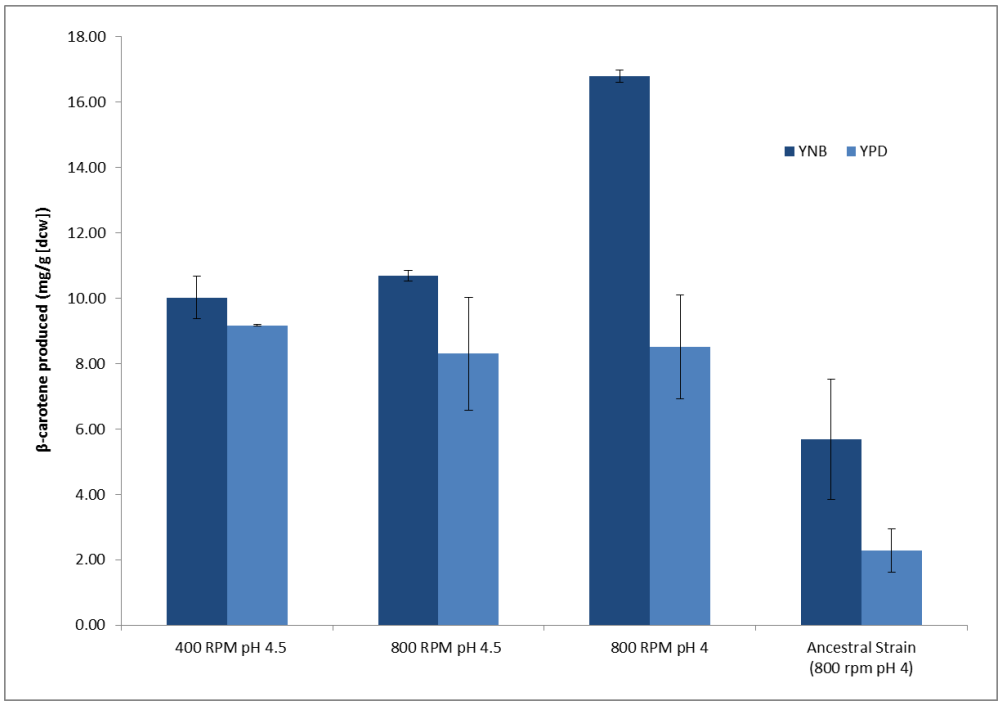

Figure 7. Effect of aeration on SM14 carotenoid production with respect to growth medium and pH.

pH is the variable that has the most affect on β-carotene production and metabolite concentrations. In YPD media, pH has very little if any affect on carotenoid production. The deviations of carotenoid production in YPD media are based on substrate irregularities, specifically in yeast extract. YNB media, however, responds to pH fluctuations and the results are consistent between each replicate of specific run conditions. The natural pH of the carotenoid *S. cerevisiae* yeast cultures in the bioreactor is around pH 3.0. β-carotene production in YNB media is highest at pH 4.0 and production decreases as pH increases, as shown in Figures 7 and 8. In YNB media at pH 4.5 and 5.0, glucose exhaustion happens around 12 hours and ethanol consumption ends around 24-30 hours. In YNB media at pH 4.0, metabolite analysis reveals a trend of slower glucose and ethanol consumption in comparison to the higher pH counterparts. Both glucose and ethanol took twice as long to be consumed: glucose in around 24 hours

and ethanol in around 60 hours. This trend was seen in other isolated mutants from the two different populations (SM12 and SM22) as well as the ancestral strain (YLH2) runs. SM12 is from the same population as SM14 and SM22 is from a separate evolved population [53], demonstrating that the metabolic profile result is consistent across different genetic backgrounds.

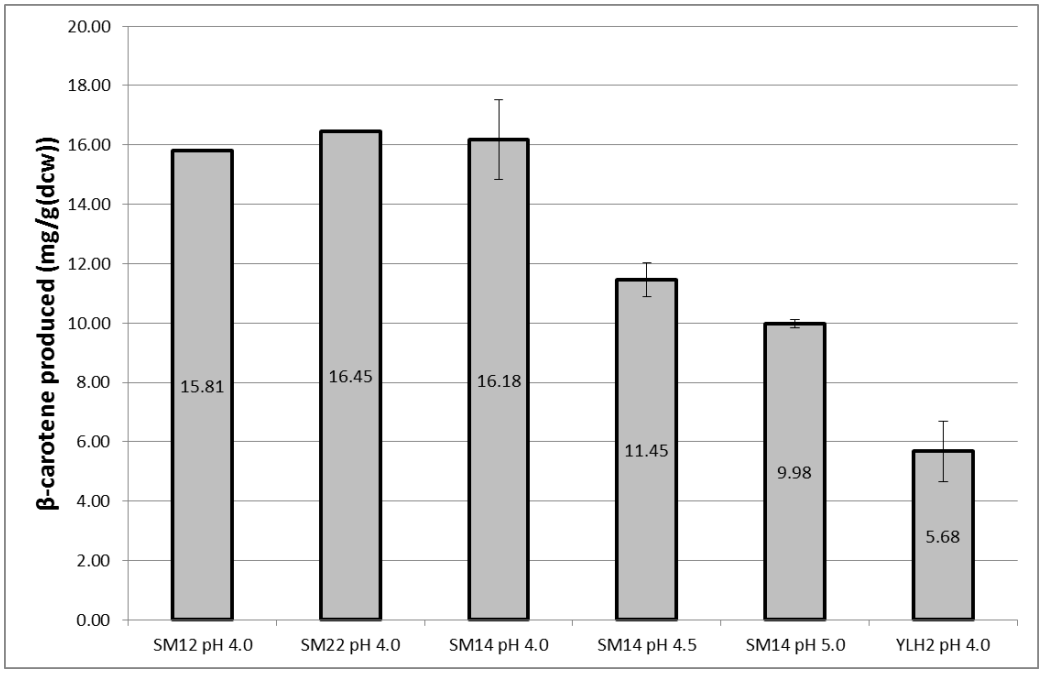

Figure 8. Maximum β-carotene produced in batch bioreactor. Agitation at 800 rpm, YNB medium, 72 h run time.

Acetic acid, which was another measured metabolite, also had varying concentrations throughout the run time and differed between runs of different parameters. At 400 rpm there is an observed spike in acetic acid concentration by hour 60, which is reproducible across all runs at 400 rpm and different media types. By 60 hours the ethanol is depleted, acetate concentration rises, and the β-carotene productivity rate increases as seen in Figure 9. Acetate concentrations in YPD batch runs with an agitation of 800 rpm stay

around 2-4 mM and there is not a very clear trend for correlating acetate to carotenoid production levels. In YNB media with 800 rpm agitation and pH range of 4 to 5, the acetate concentration increases with carotenoid production levels. After 12-18 hours post ethanol depletion, the acetate is consumed and the bioreactor biomass reaches a maximum, as seen in Figure 9. This phenomenon is observed in SM14, the ancestral strain YLH2, and the two other isolated single mutants tested (SM12 and SM22).

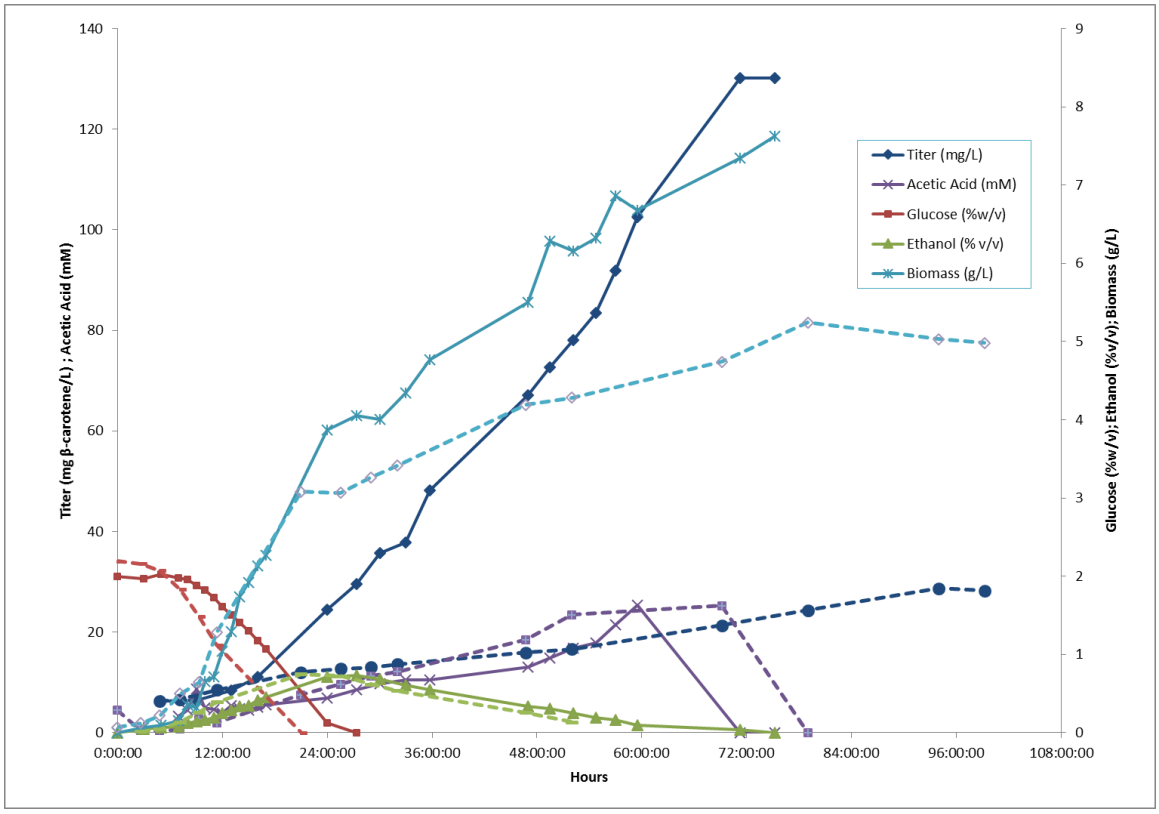

Figure 9. Carotenoid titer, biomass, and metabolite comparison of YNB batch run of SM14 and YLH2 (ancestral strain). 800 rpm, pH 4. ----: denotes ancestral strain values.

4.2 Metabolic engineering of *S. cerevisiae*

In previous work, the CTT1 catalase gene was removed from the genome in order to have more effective hydrogen peroxide shock experiments. The removal of the CTT1 gene reduced carotenoid expression in the unevolved ancestral strain by ~43% decrease [53]. To test whether carotenoid levels would increase with the CTT1 gene back in the genome, we reintegrated CTT1 into the isolated single mutant SM14 and the ancestral strain YLH2. What we saw was that reintroduction of CTT1 increased β-carotene titer only in the SM14 strain. The increase was from 15.1 ± 3.25 mg/g [dcw] to 22 ± 2.1 mg/g [dcw], as seen in Figure 10.

The second aim to further increase carotenoid production in our strains utilized metabolic engineering to introduce tHMG1, which is the known rate-limiting step in the mevalonate pathway. To our surprise, overexpression of tHMG1 did not substantially increase β-carotene production in the strains. The presence of the empty plasmid in the strains also reduced carotenoid production, as seen in Figure 10. This may demonstrate that the self-replicating plasmid poses a metabolic burden on the cell and negatively influences carotenoid production.

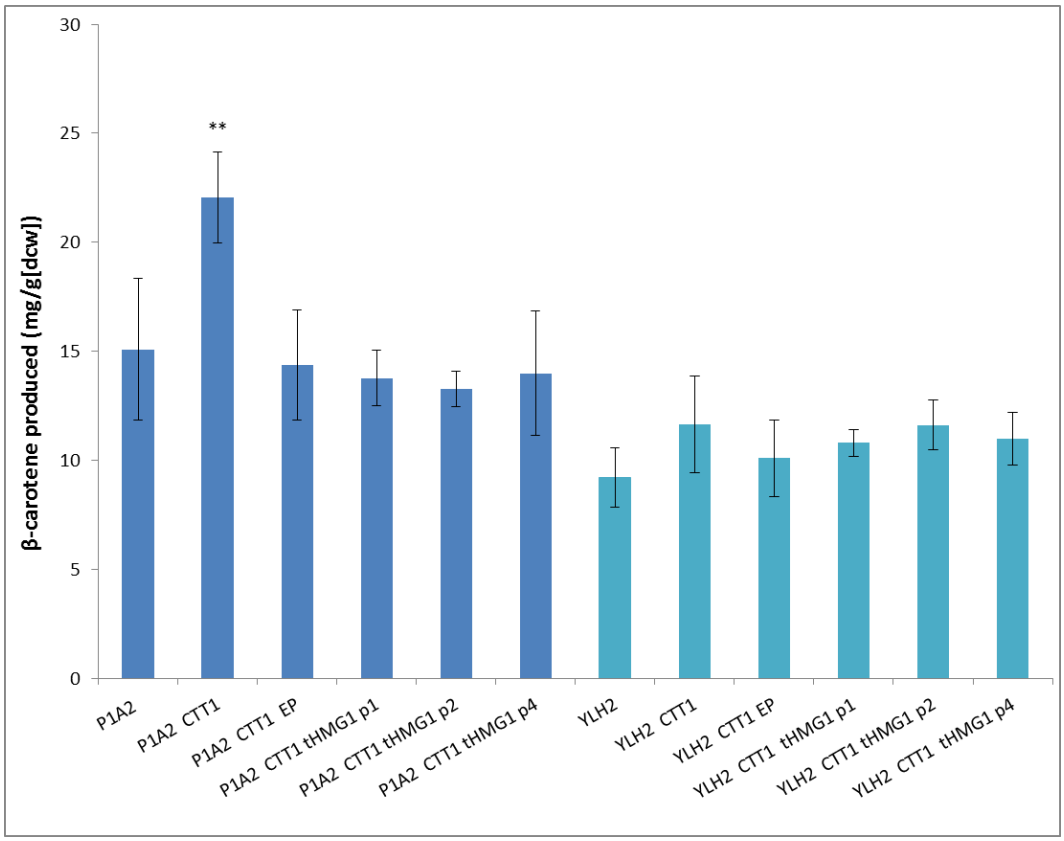

Figure 10. β-carotene quantification comparison between strains with tHMG1 and CTT1. All strains were in 3 ml YPD cultures grown at 30°C for 72 hours. EP: empty plasmid control. tHMG1 p1, p2, p4: "p" represents plasmid and 1, 2, 4 are three different isolated transformants with the tHMG1 overexpression plasmid construction. Each strain contains at least three biological replicates. ** = $p < 0.01$; (two-tailed Student's t-test with unequal variance).

5. DISCUSSION

Yeast cells are exposed to a multitude of stress and metabolic challenges through industrial fermentation. There are physical stresses such as pressure and cell shearing, and chemical stresses in the form of osmotic shock, oxidative stress, and feedstock, metabolite, and product toxicities [28]. Increased stress has been shown to effect the metabolic activity and longevity of yeast, which ultimately hinders fermentation performance [28]. Both redox homeostasis and cell rescue/defense/virulence were found to be functionally enriched in the initial stages of fermentation. Both of these functions use genes involved in oxidative stress protection [28]. The ergosterol biosynthesis pathway, which has the same precursors as the carotenoid biosynthesis pathway, is highly connected to oxidative stress of the cell. A deficiency in ergosterol production elevates oxidative stress in yeast, demonstrating the importance of a well-functioning mevalonate pathway for cellular homeostasis [28, 58, 59].

The main objective of this work was to increase β-carotene production in our isolated hyper-producer carotenoid *S. cerevisiae* strains. The first goal was to optimize the growth conditions in the bioreactor to determine which parameters most affect β-carotene production. Despite the similar metabolic profiles of the evolved mutants and the ancestral strain, there is a very drastic difference in the β-carotene titer productivity rates between the two strains. In the evolved mutants, from the initial start of fermentation and consistently throughout the run, there is a large positive upward slope of β-carotene production. The β-carotene production in the ancestral strain appears to stay at a near constant level within a 72-hour fermentation, as seen in Figure 9. Studies have shown an enriched cellular defense response in the initial hours of fermentation [28], which in combination with our evolved strains may encourage the higher productivity rates.

We found that metabolite concentrations in the bioreactor are somewhat dependent on media composition, agitation, and pH. The different parameters and resulting metabolic profiles also reflect the extent of β-carotene production in the cell. In our experiments, a dramatic increase in the production of β-carotene occurs after the glucose substrate has been consumed. A similar trend was seen in a study using *S. cerevisiae* for bisabolene production, which used the same pathway and precursor enzymes as those for β-carotene production [15]. During the time of glucose exhaustion and the beginning of ethanol consumption at around 12 hours, the carotenoid titer undergoes a dramatic shift towards higher productivity rates. Research has correlated ethanol and acetate concentration to increased activity in the isoprenoid pathway in yeast [19]. Ethanol enhances the activity of HMG-CoA reductase and increases the amount of mevalonate in the cell. Acetate is the precursor to acetyl-CoA, which is the center of cellular metabolism and is also the first compound of the MVA pathway. If both ethanol and acetate increase the activity of the MVA pathway, there will be an increase in the activity of the pathway enzymes and accumulation of the pathway precursor compounds. This heightened activity translates to increased formation of the downstream products of the MVA pathway such as β-carotene.

The second approach to increase β-carotene production was through metabolic engineering of our yeast strains. Reintroduction of the cytosolic catalase T (CTT1) gene and overexpressing the truncated HMG1gene provided varied results for β-carotene production in our strains. It has been previously demonstrated in *E. coli* that the isoprenoid pathway is a complex phenotype and that combinations of gene deletions or expressions have the potential to increase lycopene production [17]. This complexity may also be seen in our carotenoid strains for the production of β-carotene. When CTT1 was reintroduced into YLH2 and SM14, only SM14 responded with an increase in β-carotene. It may be possible that catalase reduces oxidative stress in the cell, which then prevents oxidation of the carotenoids [37]. However, the reintroduction of CTT1 into the

ancestral strain did not increase carotenoids production; the reason for the different observations between the two strains is currently not known.

To further increase the fatty acid content and carotenoid content of the cell, tHMG1 was overexpressed on a self-replicating CEN plasmid. The transformation of the plasmid was only stable with the yeast strains containing CTT1 (YLH1). For strains lacking CTT1 (such as the hyper-producers and the ancestral strain), the transformation did not work and either the cells did not grow or they were petites. Once the CTT1 gene was reintroduced into the strains, only then was the transformation successful. The reason for this result is still unknown. The carotenoid hyper-producer SM14 with CTT1 does not respond to overexpression of tHMG1, which has been previously shown to increase β-carotene production in *S. cerevisiae* by over 400% when the gene was integrated into the yeast genome [10]. An explanation for our negative result may be a gene dosage effect or that the CEN plasmid creates excess metabolic burden on the cell [49].

Our mutant strain SM14 produces the highest amount of β-carotene in *S. cerevisiae* reported to date [10], 18 ± 1 mg/g [dcw] β-carotene compared to the current highest reported value of 5.9 mg/g [dcw]. There are other routes currently under investigation to further improve β-carotene production in yeast. One route is the fatty acid β-oxidation pathway. This pathway is not directly involved in the mevalonate pathway and includes genes involved in fatty acid synthesis as well as genes involved in the degradation of fatty acids. Indeed, more thorough investigation is needed in order to optimize our strains for carotenoid production.

6. CONCLUSIONS

Carotenoid production in *S. cerevisiae* is of a complex phenotype. The goal of our experiments was to increase the β-carotene production of our current hyper-producer strains. We targeted two aspects: optimizing growth conditions in the bioreactor and metabolically engineering the mevalonate pathway in our strains. We determined the effect of various bioreactor parameters on β-carotene production in our hyper-producer SM14 mutant strain that included aeration, pH, and media composition. Dissolved oxygen content inside the bioreactor influenced the profile of carotenoid production, but final titer of carotenoids was independent of the aeration. The pH level only influenced batch runs using defined media (YNB), where runs at pH 4 resulted in β-carotene production of 16.2 ± 1.4 mg/g [dcw] and pH 5 resulted in lower β-carotene production at 10 ± 0.1 mg/g [dcw]. The cytosolic catalase T (CTT1) gene was reintegrated back into the yeast genome; however, improvement in β-carotene production was only observed in SM14 and not the ancestral strain. Overexpression of the bottleneck HMG1 in the MVA pathway did not increase carotenoid production in the strains, suggesting that there may be a gene dosage effect or the introduced CEN plasmid creates too high of a metabolic burden on the cell. This work demonstrates that bioreactor culture parameters as well as genome manipulations influence the production of carotenoids in *S. cerevisiae*.

REFERENCES

1. Chemler, J.A., Y. Yan, and M.A. Koffas, *Biosynthesis of isoprenoids, polyunsaturated fatty acids and flavonoids in Saccharomyces cerevisiae.* Microb Cell Fact, 2006. **5**: p. 20.
2. Keasling, J.D., *Manufacturing molecules through metabolic engineering.* Science, 2010. **330**: p. 1355-8.
3. Ajikumar, P.K., et al., *Isoprenoid pathway optimization for Taxol precursor overproduction in Escherichia coli.* Science, 2010. **330**(6000): p. 70-4.
4. Asadollahi, M.A., et al., *Enhancing sesquiterpene production in Saccharomyces cerevisiae through in silico driven metabolic engineering.* Metabolic Engineering, 2009. **11**: p. 328-334.
5. Buijs, N.A., V. Siewers, and J. Nielsen, *Advanced biofuel production by the yeast Saccharomyces cerevisiae.* Curr Opin Chem Biol, 2013. **17**(3): p. 480-8.
6. Farhi, M., et al., *Harnessing yeast subcellular compartments for the production of plant terpenoids.* Metab Eng, 2011. **13**(5): p. 474-81.
7. Zhao, J., et al., *Engineering central metabolic modules of Escherichia coli for improving rpenoids.drivenuction.* Metabolic Engineering, 2013. **17**(0): p. 42-50.
8. Yuan, J. and C.B. Ching, *Combinatorial engineering of mevalonate pathway for improved amorpha-4,11-diene production in budding yeast.* Biotechnol Bioeng, 2014. **111**(3): p. 608-17.
9. Li, X., et al., *Overproduction of fatty acids in engineered Saccharomyces cerevisiae.* Biotechnol Bioeng, 2014.
10. Verwaal, R., et al., *High-level production of beta-carotene in Saccharomyces cerevisiae by successive transformation with carotenogenic genes from Xanthophyllomyces dendrorhous.* Appl Environ Microbiol, 2007. **73**(13): p. 4342-50.
11. Kampranis, S.C. and A.M. Makris, *Developing a yeast cell factory for the production of terpenoids.* Comput Struct Biotechnol J, 2012. **3**: p. e201210006.

12. Maury, J., et al., *Microbial Isoprenoid Production: An Example of Green Chemistry through Metabolic Engineering.* 2005. **100**: p. 19-51.
13. Sacchettini, J.C. and C.D. Poulter, *Creating Isoprenoid Diversity.* Science, 1997. **277**.
14. Penuelas, J. and S. Munne-Bosch, *Isoprenoids: an evolutionary pool for photoprotection.* Trends Plant Sci, 2005. **10**(4): p. 166-9.
15. Ozaydin, B., et al., *Carotenoid-based phenotypic screen of the yeast deletion collection reveals new genes with roles in isoprenoid production.* Metab Eng, 2013. **15**: p. 174-83.
16. Armstrong, G.A. and J.E. Hearst, *Genetics and molecular biology of carotenoid pigment biosynthesis.* Carotenoids 2, 1996. **10**: p. 228-237.
17. Alper, H., K. Miyaoku, and G. Stephanopoulos, *Construction of lycopene-overproducing E. coli strains by combining systematic and combinatorial gene knockout targets.* Nat Biotechnol, 2005. **23**(5): p. 612-6.
18. Yan, G.-l., et al., *Important Role of Catalase in the Production of trains by combining systematic and combinatorial gene knockout target* Current Microbiology, 2011. **62**(3): p. 1056-1061.
19. Holstein, S.A. and R.J. Hohl, *Isoprenoids: Remarkable Diversity of Form and Function.* Lipids, 2004. **39**(4): p. 293-309.
20. Caspi R, et al., *The MetaCyc database of metabolic pathways and enzymes and the BioCyc collection of pathway/genome databases.* Nucleic Acids Research, 2010. **38**: p. D473-9.
21. Bucher, N.L.R., et al., *Cholesterol Biosynthesis in Preparations of Liver from Normal, Fasting, X-irradiated, Cholesterol-fed, Triton, or Δ4 -Cholesten-3-one-treated Rats.* J. Biol. Chem., 1959. **234**: p. 262-267.
22. Siperstein, M.D. and V.M. Fagan, *Feedback Control of Mevalonate Synthesis by Dietary Cholesterol.* J. Biol. Chem., 1966. **241**: p. 602-609.

23. Wang, G. and J.D. Keasling, *Amplification of HMG-CoA Reductase Production Enhances Carotenoid Accumulation in Neurospora crassa.* Metabolic Engineering, 2002. **4**(3): p. 193-201.
24. Tholl, D., *Terpene synthases and the regulation, diversity and biological roles of terpene metabolism.* Curr Opin Plant Biol, 2006. **9**(3): p. 297-304.
25. Zhang, F.L. and P.J. Casey, *PROTEIN PRENYLATION: Molecular Mechanisms and Functional Consequences.* Annu. Rev. Biochem., 1996. **65**: p. 241-69.
26. Jones, M.B., et al., *Structure and synthesis of polyisoprenoids used in N-glycosylation across the three domains of life.* Biochim Biophys Acta, 2009. **1790**(6): p. 485-94.
27. Kawamukai, M., *Biosynthesis and bioproduction of coenzyme Q10 by yeasts and other organisms.* Biotechnol Appl Biochem, 2009. **53**(Pt 4): p. 217-26.
28. Higgins, V.J., et al., *Yeast Genome-Wide Expression Analysis Identifies a Strong Ergosterol and Oxidative Stress Response during the Initial Stages of an Industrial Lager Fermentation.* Applied and Environmental Microbiology, 2003. **69**(8): p. 4777-4787.
29. Zinser, E., F. Paltauf, and G. Daum, *Sterol composition of yeast organelle membranes and subcellular distribution of enzymes involved in sterol metabolism.* Journal of Bacteriology, 1993. **175**(10): p. 2853-2858.
30. Farrugia, G. and R. Balzan, *Oxidative stress and programmed cell death in yeast.* Frontiers in Oncology, 2012. **2**.
31. Drakulic, T., et al., *Involvement of oxidative stress response genes in redox homeostasis, the level of reactive oxygen species, and ageing in Saccharomyces cerevisiae.* FEMS Yeast Res, 2005. **5**(12): p. 1215-28.
32. Perrone, G.G., S.X. Tan, and I.W. Dawes, *Reactive oxygen species and yeast apoptosis.* Biochim Biophys Acta, 2008. **1783**(7): p. 1354-68.
33. Jamieson, D.J., *Oxidative Stress Responses of the Yeast Saccharomyces cerevisiae.* Yeast, 1998. **14**: p. 1511-1527.

34. Yazawa, H., et al., *Production of polyunsaturated fatty acids in yeast Saccharomyces cerevisiae and its relation to alkaline pH tolerance.* Yeast, 2009. **26**(3): p. 167-184.
35. Hill, S., et al., *Isotope-reinforced polyunsaturated fatty acids protect yeast cells from oxidative stress.* Free Radic Biol Med, 2011. **50**(1): p. 130-8.
36. Bissinger, P.H., et al., *Control of Saccharomyces cerevisiae Catalase T Gene (CTTI) Expression by Nutrient Supply via the RAS-Cyclic AMP Pathway.* Molecular and Cellular Biology, 1989. **9**(3): p. 1309-1315.
37. Watanabe, T., et al., *Requirement of peroxiredoxin on the stationary phase of yeast cell growth.* The Journal of Toxicological Sciences, 2014. **39**(1): p. 51-58.
38. Johnson, E.A. and W.A. Schroeder, *Microbial carotenoids.* Advances in biochemical engineering/biotechnology, 1996. **53**: p. 119-78.
39. Vachali, P., P. Bhosale, and P.S. Bernstein, *Microbial carotenoids.* Methods Mol Biol, 2012. **898**: p. 41-59.
40. Lee, P.C. and C. Schmidt-Dannert, *Metabolic engineering towards biotechnological production of carotenoids in microorganisms.* Appl Microbiol Biotechnol, 2002. **60**(1-2): p. 1-11.
41. *The Global Market for Carotenoids*. 2011; Available from: http://www.bccresearch.com/market-research/food-and-beverage/carotenoids-global-market-fod025d.html.
42. Bhosale, P., *Environmental and cultural stimulants in the production of carotenoids from microorganisms.* Appl Microbiol Biotechnol, 2004. **63**(4): p. 351-61.
43. Gu, W.-L., G.-H. An, and E. Johnson, *Ethanol increases carotenoid production in Phaffia rhodozyma.* Journal of Industrial Microbiology and Biotechnology, 1997. **19**: p. 114-117.
44. Ostergaard, S., L. Olsson, and J. Nielsen, *Metabolic Engineering of Saccharomyces cerevisiae.* Microbiology and Molecular Biology Reviews, 2000. **64**(1): p. 34-50.

45. Ausich, R.L., *Commercial opportunities for carotenoids production by biotechnology.* Pure and Applied Chemistry, 1997. **69**: p. 2169-2173.
46. Curran, K.A. and H.S. Alper, *Expanding the chemical palate of cells by combining systems biology and metabolic engineering.* Metabolic Engineering, 2012. **14**(4): p. 289-297.
47. Karim, A.S., K.A. Curran, and H.S. Alper, *Characterization of plasmid burden and copy number in Saccharomyces cerevisiae for optimization of metabolic engineering applications.* FEMS Yeast Research, 2013. **13**(1): p. 107-116.
48. Da Silva, N.A. and S. Srikrishnan, *Introduction and expression of genes for metabolic engineering applications in Saccharomyces cerevisiae.* FEMS Yeast Research, 2012. **12**(2): p. 197-214.
49. Wittrup, K.D., et al., *Existence of an Optimum Expression Level for Secretion of Foreign Proteins in Yeasta.* Annals of the New York Academy of Sciences, 1994. **745**(1): p. 321-330.
50. Peralta-Yahya, P.P., et al., *Identification and microbial production of a terpene-based advanced biofuel.* Nat Commun, 2011. **2**: p. 483.
51. Schmidt-Dannert, C., *Engineering novel carotenoids in microorganisms.* Current Opinion in Biotechnology, 2000. **11**: p. 255-261.
52. Kao, K.C. and G. Sherlock, *Molecular characterization of clonal interference during adaptive evolution in asexual populations of Saccharomyces cerevisiae.* Nat Genet, 2008. **40**(12): p. 1499-504.
53. Reyes, L.H., J.M. Gomez, and K.C. Kao, *Improving carotenoids production in yeast via adaptive laboratory evolution.* Metab Eng, 2014. **21**: p. 26-33.
54. Gietz, R.D., et al., *Improved method for high efficiency transformation of intact yeast cells.* Nucleic Acids Research, 1992. **20**(6): p. 1425.
55. Gietz, R.D., et al., *Studies on the Transformation of Intact Yeast Cells by the LiAc/SS-DNA/PEG Procedure.* Yeast, 1995. **11**: p. 355-360.

56. Goldstein, A.L. and J.H. McCusker, *Three New Dominant Drug Resistance Cassettes for Gene Disruption in Saccharomyces cerevisiae.* Yeast, 1999. **15**: p. 1541-1553.
57. Mata-Gómez, L.C., et al., *Biotechnological production of carotenoids by yeasts: an overview.* Microbial Cell Factories, 2014. **13**(12): p. 1-11.
58. Bammert, G.F. and J.M. Fostel, *Genome-wide expression patterns inSaccharomyces cerevisiae: comparison of drug treatments and genetic alterations affecting biosynthesis of ergosterol.* Antimicrobial agents and chemotherapy, 2000. **44**(5): p. 1255-1265.
59. Schmidt, C.L., et al., *Allelism of Saccharomyces cerevisiae genes PSO 6, involved in survival after 3 ‐ CPs+ UVA induced damage, and ERG 3, encoding the enzyme sterol C ‐ 5 desaturase.* Yeast, 1999. **15**(14): p. 1503-1510.
60. Sandoval, N.R., et al., *Elucidating acetate tolerance in E. coli using a genome-wide approach.* Metabolic Engineering, 2011. **13**(2): p. 214-224.
61. Almario, M.P., L.H. Reyes, and K.C. Kao, *Evolutionary engineering of Saccharomyces cerevisiae for enhanced tolerance to hydrolysates of lignocellulosic biomass.* Biotechnology and Bioengineering, 2013. **110**(10): p. 2616-2623.
62. Reyes, L.H., et al., *Visualizing evolution in real time to determine the molecular mechanisms of n-butanol tolerance in Escherichia coli.* Metabolic Engineering, 2012. **14**(5): p. 579-590.
63. Minty, J., et al., *Evolution combined with genomic study elucidates genetic bases of isobutanol tolerance in Escherichia coli.* Microbial Cell Factories, 2011. **10**(1): p. 18.
64. Shiloach, J. and R. Fass, *Growing E. coli to high cell density—A historical perspective on method development.* Biotechnology Advances, 2005. **23**(5): p. 345-357.

65. Dobson, R., V. Gray, and K. Rumbold, *Microbial utilization of crude glycerol for the production of value-added products.* Journal of industrial microbiology & biotechnology, 2012. **39**(2): p. 217-226.
66. Rumbold, K., et al., *Microbial production host selection for converting second-generation feedstocks into bioproducts.* Microb Cell Fact, 2009. **8**: p. 64.
67. Padan, E., et al., *Deletion of ant in Escherichia coli reveals its function in adaptation to high salinity and an alternative Na+/H+ antiporter system(s).* Journal of Biological Chemistry, 1989. **264**(34): p. 20297-20302.
68. Rozwadowski, K.L., G.G. Khachatourians, and G. Selvaraj, *Choline oxidase, a catabolic enzyme in Arthrobacter pascens, facilitates adaptation to osmotic stress in Escherichia coli.* Journal of bacteriology, 1991. **173**(2): p. 472-478.
69. Purvis, J.E., L. Yomano, and L. Ingram, *Enhanced trehalose production improves growth of Escherichia coli under osmotic stress.* Applied and environmental microbiology, 2005. **71**(7): p. 3761-3769.
70. Dragosits, M. and D. Mattanovich, *Adaptive laboratory evolution-principles and applications for biotechnology.* Microb Cell Fact, 2013. **12**: p. 64.
71. Atsumi, S., et al., *Evolution, genomic analysis, and reconstruction of isobutanol tolerance in Escherichia coli.* Molecular systems biology, 2010. **6**(1).
72. Wright, J., et al., *Batch and continuous culture‐based selection strategies for acetic acid tolerance in xylose‐fermenting Saccharomyces cerevisiae.* FEMS yeast research, 2011. **11**(3): p. 299-306.
73. Toprak, E., et al., *Evolutionary paths to antibiotic resistance under dynamically sustained drug selection.* Nature genetics, 2012. **44**(1): p. 101-105.
74. Winkler, J. and K.C. Kao, *Harnessing recombination to speed adaptive evolution in Escherichia coli.* Metabolic Engineering, 2012. **14**(5): p. 487-495.
75. Barrick, J.E., et al., *Genome evolution and adaptation in a long-term experiment with Escherichia coli.* Nature, 2009. **461**(7268): p. 1243-1247.

76. Dragosits, M., et al., *Evolutionary potential, cross‐stress behavior and the genetic basis of acquired stress resistance in Escherichia coli.* Molecular systems biology, 2013. **9**(1).
77. Typas, A., et al., *High-throughput, quantitative analyses of genetic interactions in E. coli.* Nat Meth, 2008. **5**(9): p. 781-787.
78. Achtman, M., N. Kennedy, and R. Skurray, *Cell--cell interactions in conjugating Escherichia coli: role of traT protein in surface exclusion.* Proceedings of the National Academy of Sciences, 1977. **74**(11): p. 5104-5108.
79. Baba, T., et al., *Construction of Escherichia coli K‐12 in‐frame, single‐gene knockout mutants: the Keio collection*. Vol. 2. 2006.
80. Kitagawa, M., et al., *Complete set of ORF clones of Escherichia coli ASKA library (a complete set of E. coli K-12 ORF archive): unique resources for biological research.* DNA research, 2006. **12**(5): p. 291-299.
81. Datsenko, K.A. and B.L. Wanner, *One-step inactivation of chromosomal genes in Escherichia coli K-12 using PCR products.* Proceedings of the National Academy of Sciences, 2000. **97**(12): p. 6640-6645.
82. Winkler, J.D., et al., *Evolved Osmotolerant Escherichia coli Mutants Frequently Exhibit Defective N-Acetylglucosamine Catabolism and Point Mutations in Cell Shape-Regulating Protein MreB.* Applied and Environmental Microbiology, 2014. **80**(12): p. 3729-3740.
83. Young, K., *In vitro antibacterial resistance selection and quantitation.* Current Protocols in Pharmacology, 2006: p. 13A. 6.1-13A. 6.22.
84. Winkler, J. and K.C. Kao, *Transcriptional analysis of Lactobacillus brevis to N-butanol and ferulic acid stress responses.* PloS one, 2011. **6**(8): p. e21438.
85. Domka, J., J. Lee, and T.K. Wood, *YliH (BssR) and YceP (BssS) Regulate Escherichia coli K-12 Biofilm Formation by Influencing Cell Signaling.* Applied and Environmental Microbiology, 2006. **72**(4): p. 2449-2459.

86. Genevaux, P., S. Muller, and P. Bauda, *A rapid screening procedure to identify mini‐Tn10 insertion mutants of Escherichia coli K‐12 with altered adhesion properties.* FEMS microbiology letters, 1996. **142**(1): p. 27-30.
87. Conrad, T.M., et al., *RNA polymerase mutants found through adaptive evolution reprogram Escherichia coli for optimal growth in minimal media.* Proceedings of the National Academy of Sciences, 2010. **107**(47): p. 20500-20505.
88. Reyes, L.H., A.S. Abdelaal, and K.C. Kao, *Genetic Determinants for n-Butanol Tolerance in Evolved Escherichia coli Mutants: Cross Adaptation and Antagonistic Pleiotropy between n-Butanol and Other Stressors.* Applied and environmental microbiology, 2013. **79**(17): p. 5313-5320.
89. Cullum, A.J., A.F. Bennett, and R.E. Lenski, *Evolutionary adaptation to temperature. IX. Preadaptation to novel stressful environments of Escherichia coli adapted to high temperature.* Evolution, 2001. **55**(11): p. 2194-2202.
90. Vollmer, W., D. Blanot, and M.A. De Pedro, *Peptidoglycan structure and architecture.* FEMS microbiology reviews, 2008. **32**(2): p. 149-167.
91. Holmes, R.P. and R.R.B. Russell, *Mutations Affecting Amino Sugar Metabolism in Escherichia coli K-12.* Journal of Bacteriology, 1972. **111**(1): p. 290-291.
92. Vats, P., Y.L. Shih, and L. Rothfield, *Assembly of the MreB‐associated cytoskeletal ring of Escherichia coli.* Molecular microbiology, 2009. **72**(1): p. 170-182.
93. Ishino, F., et al., *Peptidoglycan synthetic activities in membranes of Escherichia coli caused by overproduction of penicillin-binding protein 2 and rodA protein.* Journal of Biological Chemistry, 1986. **261**(15): p. 7024-31.
94. Shiomi, D., et al., *Mutations in cell elongation genes mreB, mrdA and mrdB suppress the shape defect of RodZ‐deficient cells.* Molecular microbiology, 2013. **87**(5): p. 1029-1044.
95. Snyder, J.A., et al., *Transcriptome of Uropathogenic Escherichia coli during Urinary Tract Infection.* Infection and Immunity, 2004. **72**(11): p. 6373-6381.

96. Kempf, B. and E. Bremer, *Uptake and synthesis of compatible solutes as microbial stress responses to high-osmolality environments.* Archives of microbiology, 1998. **170**(5): p. 319-330.
97. Toba, F.A., et al., *Role of DLP12 lysis genes in Escherichia coli biofilm formation.* Microbiology, 2011. **157**(6): p. 1640-1650.
98. Punta, M., et al., *The Pfam protein families database.* Nucleic Acids Research, 2012. **40**(D1): p. D290-D301.
99. Keseler, I.M., et al., *EcoCyc: fusing model organism databases with systems biology.* Nucleic Acids Research, 2013. **41**(D1): p. D605-D612.
100. Hase, Y., et al., *Impairment of ribosome maturation or function confers salt resistance on Escherichia coli cells.* PloS one, 2013. **8**(5): p. e65747.
101. Hobbs, E.C., et al., *Conserved small protein associates with the multidrug efflux pump AcrB and differentially affects antibiotic resistance.* Proceedings of the National Academy of Sciences, 2012. **109**(41): p. 16696-16701.
102. Verheul, A., et al., *A possible role of ProP, ProU and CaiT in osmoprotection of Escherichia coli by carnitine.* Journal of applied microbiology, 1998. **85**(6): p. 1036-1046.
103. Lucht, J.M. and E. Bremer, *Adaptation of< i> Escherichia coli</i> to high osmolarity environments: Osmoregulation of the high-affinity glycine betaine transport system ProU.* FEMS microbiology reviews, 1994. **14**(1): p. 3-20.
104. Khodursky, A.B., et al., *DNA microarray analysis of gene expression in response to physiological and genetic changes that affect tryptophan metabolism in Escherichia coli.* Proceedings of the National Academy of Sciences, 2000. **97**(22): p. 12170-12175.
105. Lee, J.H. and J. Lee, *Indole as an intercellular signal in microbial communities.* FEMS microbiology reviews, 2010. **34**(4): p. 426-444.
106. Barnhart, M.M., J. Lynem, and M.R. Chapman, *GlcNAc-6P Levels Modulate the Expression of Curli Fibers by Escherichia coli.* Journal of Bacteriology, 2006. **188**(14): p. 5212-5219.

107. Sohanpal, B.K., et al., *Integrated regulatory responses of fimB to N-acetylneuraminic (sialic) acid and GlcNAc in Escherichia coli K-12.* Proceedings of the National Academy of Sciences of the United States of America, 2004. **101**(46): p. 16322-16327.

108. Ma, Z., N. Masuda, and J.W. Foster, *Characterization of EvgAS-YdeO-GadE Branched Regulatory Circuit Governing Glutamate-Dependent Acid Resistance in Escherichia coli.* Journal of Bacteriology, 2004. **186**(21): p. 7378-7389.

109. Russo, F.D., J.M. Slauch, and T.J. Silhavy, *Mutations that Affect Separate Functions of OmpR the Phosphorylated Regulator of Porin Transcription in< i> Escherichia coli</i>.* Journal of molecular biology, 1993. **231**(2): p. 261-273.

110. Fogle, C.A., J.L. Nagle, and M.M. Desai, *Clonal Interference, Multiple Mutations and Adaptation in Large Asexual Populations.* Genetics, 2008. **180**(4): p. 2163-2173.

111. Sniegowski, P.D. and P.J. Gerrish, *Beneficial mutations and the dynamics of adaptation in asexual populations.* Philosophical Transactions of the Royal Society B: Biological Sciences, 2010. **365**(1544): p. 1255-1263.

APPENDIX*

1. Evolved Osmotolerant Escherichia coli Mutants Frequently Exhibit Defective N-Acetylglucosamine Catabolism and Point Mutations in Cell Shape-Regulating Protein MreB. Winkler, J., C. Garcia, M. Olson, E. Callaway, and K. C. Kao. Appl. Environ. Microbiol. 2014, 80(12): 3729-3740.

Escherichia coli, an important industrial microorganism for the production of a wide variety of fine chemicals, fuels, and proteins, has been extensively targeted to improve its suitability as a biofactory. Strain development efforts have focused on improving tolerance of feedstocks containing toxic compounds [60, 61] or products [62, 63]. Many environmental variables, including osmotic pressure, can negatively impact biocatalyst performance [64]. Use of nonconventional waste streams, such as waste glycerol or brackish water sources, to support microbial growth can also reduce process costs [65, 66] while reducing pressure on fresh water resources; however, these carbon and water sources generally contain high concentrations of salt that may be inhibitory to microbial growth. In addition to osmotic stresses, excess Na^+ can disrupt the ion homeostasis in *E. coli* as well [67]. Previous studies have attempted to engineer improved osmotic tolerance in *E. coli* [68, 69], but overall, knowledge of the genetic mechanisms that confer tolerance of osmotic stress in general or to specific osmolytes remains limited. A detailed analysis of *E. coli* osmotolerance to osmolytes would therefore provide new insight into the molecular mechanisms underlying this complex phenotype.

Adaptive laboratory evolution [70] is a promising approach to identify potentially novel osmotic tolerance mechanisms, as this technique requires no assumptions about the

*Reprinted with permission from "Evolved Osmotolerant Escherichia coli Mutants Frequently Exhibit Defective N-Acetylglucosamine Catabolism and Point Mutations in Cell Shape-Regulating Protein MreB" by Winkler, J., C. Garcia, M. Olson, E. Callaway, and K. C. Kao, 2014. *Appl. Environ. Microbiol.*, 80(12): 3729-3740, Copyright [2014] by American Society for Microbiology.

underlying genotype-phenotype relationship. Complex phenotypes, such as enhanced resistance to biofuels [62, 63, 71], lignocellulosic hydrolysates [61, 72], antibiotics [73, 74], and environmental conditions [75], have all been successfully characterized using this approach. In this study, sodium chloride (NaCl) was selected as the osmotic inhibitor. A recent evolutionary study aimed at characterizing cross-adaptation between several different stressors detected several potential mechanisms in a single evolved NaCl-tolerant isolate [76], but due to the possible existence of multiple adaptation mechanisms, additional information is needed to better understand the genetic bases of osmotolerance.

In order to identify novel genetic mechanisms for osmotic (NaCl) tolerance, we have utilized adaptive laboratory evolution to generate osmotic-tolerant mutants of two distinct *E. coli* strains: one capable of *in situ* recombination to reduce clonal interference between osmotolerant mutants and another, completely asexual strain [74]. These strains will enable a comparison between the sexual evolution system and typical evolutionary engineering approaches for an industrially relevant phenotype. After being propagated for approximately 150 generations in the presence of increasing concentrations of NaCl, osmotolerant mutants were isolated, characterized, and sequenced to identify any genetic changes that occurred during evolution. The elucidated resistance mechanisms were then explored phenotypically to better understand their potential impact on *E.coli* physiology. Transcriptomic analyses of several mutants were subsequently conducted to better characterize the genotype-phenotype connection that resulted in enhanced osmotolerance.

MATERIALS AND METHODS

Bacterial strains and growth media. All strains used for evolution in this study were previously developed BW25113 derivatives [74]. Briefly, Hfr-2xSFX− is a conjugation-

proficient, surface exclusion-deficient Hfr strain with an operon of F transfer proteins integrated at the *trp* locus [77]. Recombination is therefore more frequent for the Hfr-2xSFX− strain than for an Hfr strain with intact surface exclusion, which acts to prevent redundant transfer between Hfr and F+ strains [78]. 2xOriT, an F− strain, was used as an asexual control. Knockout strains were obtained from the Keio collection [79], while ASKA overexpression plasmids were transformed into BW25113 from the original AG1 host [80] for both overexpression and compensatory assays. The kanamycin resistance marker in the Keio strains was also removed by transformation with pCP20 as needed for strain construction and screening [81]. The full list of strains and plasmids used in this study is given in Table S1 in the supplemental material. Minimal M9 medium supplemented with 0.5% (wt/vol) glucose and 50 μg/ml tryptophan [74, 77] was used for routine cultivation and growth assays, while Luria-Bertani (LB) broth and agar plates were used for strain isolation, transformation, and other analyses where indicated. Sodium chloride (JT Baker) was utilized to adjust the osmotic strength of the medium during the evolution and for subsequent growth assays.

Evolution experiment. Adaptive laboratory evolution was conducted via serial batch transfer experiments to improve the osmotic stress tolerance of Hfr-2xSFX− and 2xOriT in parallel. Six replicate populations for each strain were inoculated from independent colonies to initiate the evolution experiment in 0.55 M (32 g/liter) NaCl and increased to 0.6 M (35 g/liter) NaCl after one serial transfer. Approximately every 24 h, a proportion (typically 1 to 3%, based on cell density) of each replicate population was diluted into fresh medium to ensure that each population underwent approximately 6 or 7 generations per transfer for a total of 150 generations. Sodium chloride concentrations were periodically increased from 0.6 M to 0.75 M (32 to 35 to 44 g/liter), as fitness increases were observed in population level data every 24 generations (Fig. 1); the daily concentration of NaCl in each replicate set is shown in Fig. S1 in the supplemental material. The initial NaCl concentration was chosen to reduce the growth rates of the ancestral strains by approximately 50%. The fitness (*S*; equation 1) of the evolving

populations relative to their ancestral parents was determined every 24 generations using growth assays in microtiter plates to track their rates of adaptation; 0.6 M (35 g/liter) NaCl was used for the initial fitness measurement at generation zero to account for the lower initial tolerance of the Hfr strains, and 0.65 M (38 g/liter) NaCl was used thereafter. The specific growth rate (μ) was calculated by linearizing the measured growth curves and calculating the slope in exponential growth phase using standard regression procedures. The subscript *i* refers to the measured growth rate for the *i*th population or mutant under investigation.

A logarithmic model (equation 2) was then fitted to the fitness measurements (S; see below) for each population and used to calculate their overall rate of improvement throughout the evolution experiment based on the expected shape of the improvement curve [75], where the constant α is a shape parameter for the logarithmic curve. The variable *t* refers to the number of generations that have occurred since the initial inoculation of the experiment. Potential external contamination and cross-contamination of the experiment were monitored as described by Winkler and Kao [74].

$$S = \frac{\mu_i}{\mu_{2xoriT}} - 1 \quad (1)$$

$$S(t) = \alpha \log(t) \quad (2)$$

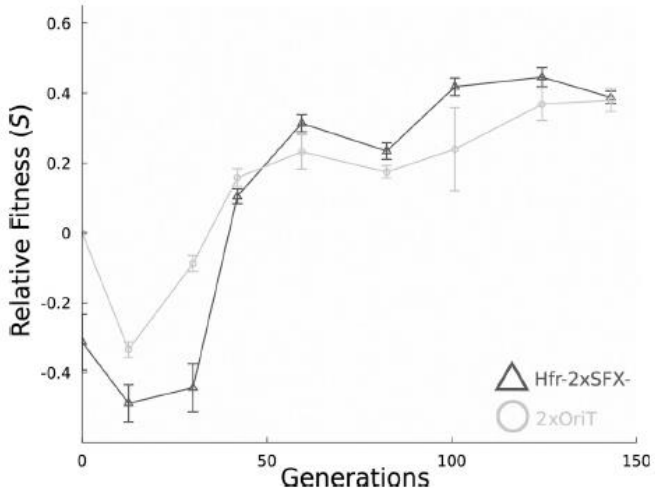

Figure 1. Average fitness improvements for the Hfr-2xSFX− and 2xOriT populations, relative to the 2xOriT parent strain during evolution in the presence of high sodium chloride concentrations. NaCl concentrations used during fitness assays were 0.6 M (35 g/liter) for the first measurement and 0.65 M (38 g/liter) for all subsequent measurements. Fitness is defined as $S = \mu pop/\mu 2xOriT - 1$ in this case, where pop refers to the population average growth rate for each evolving population under NaCl challenge. Error bars are 95% confidence intervals using the Student t distribution [82].

Mutant isolation and screening. One clonal isolate was randomly obtained from each evolved population (to ensure mutational independence) at the end of the evolution experiment after streaking the evolved populations onto LB agar for single colonies. Isolates from the Hfr- 2xSFX− and 2xOriT populations are prefaced with G and A, respectively. All isolates were propagated in M9 minimal medium without excess NaCl for at least 10 generations prior to any phenotypic analysis. All cultures were grown in glucose minimal medium with tryptophan overnight and diluted 100-fold (optical density at 600 nm [OD600] ≈ 0.04) into medium containing various stressors for growth over 24 to 36 h. Cross-adaptation was analyzed using several general stress conditions (excess glucose [54 g/liter], *n-butanol* [0.8% vol/vol], mild acid stress pH [pH = 6.0], or elevated temperature [42°C]) with two biological and 4 technical replicates per strain per condition. While these stressors would be more severe in an industrial fermenter, the purpose of this assay is to analyze incidental phenotypic changes associated with osmotic tolerance. All growth assays were performed in 96-well microtiter plates using a plate shaker and incubator (TECAN Infinite M200) at 37°C (except for thermal stress assays). Relative fitness (S) and improvement (RI) of the *ith* mutant were, respectively, calculated for each condition using equations 1 and 3. Subscripts *C* and *U* refer to challenged and unchallenged maximum growth rates, respectively, where *C* can be any of the stress conditions listed above and sodium chloride stress.

Fitness assays for knockout, overexpression, and compensatory assays were conducted in screw-cap tubes with 5 ml of M9 minimal medium, supplemented with glucose,

tryptophan, and 0.55 M (32 g/liter) NaCl. A lower concentration of NaCl was used for these assays to permit gathering of a full growth curve within 24 h. OD600 readings were taken every 2 h until exponential growth had been sustained for at least 3 doublings. Fitness of the overexpression and knockout strains relative to the appropriate references (empty vector controls for the overexpression strains, BW25113 for knockout strains) was then calculated using equation 1. Three biological replicates per strain were analyzed.

$$RI = \frac{\mu_{i,C}/\mu_{i,U}}{\mu_{2xOriT,C}/\mu_{2xOriT,U}} - 1 \quad (3)$$

Fitness distribution analysis. Six randomly isolated clones were obtained by streaking from each of the evolved Hfr-2xSFX− and 2xOriT replicate populations (for a total of 36 random isolates per strain). Each colony was inoculated into 2 ml glucose minimal medium supplemented with tryptophan and allowed to grow for 24 h. The fitness of each isolate (relative to 2xOriT) was then determined using growth in a microtiter plate under 0.65 M (38 g/liter) NaCl challenge, as described previously. Four technical replicates were used per screened isolate.

Mutation rate under osmotic stress. The mutation rates of Hfr- 2xSFX− and 2xOriT were measured using a standard fluctuation test [83] under 0.55 M (32 g/liter) NaCl stress to determine if the strains have unequal mutation rates under osmotic stress, which would influence their relative adaptation rates. For 2xOriT, the mutation rate is 1.43 mutants per 109 cells (95% confidence interval of 0.72 to 2.31); for Hfr-2xSFX−, the mutation rate is 1.52 mutants per 109 cells (95% confidence interval of 0.71 to 2.54). The difference in mutation rate between the strains is not statistically significant.

Hyperosmotic shock tests. Single colonies of each isolate (G1 to G6 and A1 to A6) and the parental controls were inoculated into glucose minimal medium and allowed to grow overnight. The stationary-phase cultures were then diluted in fresh medium and

propagated until mid- exponential phase (OD600 ≈ 0.3 to 0.6). The cultures were then normalized to equivalent optical densities, pelleted, and resuspended in glucose minimal medium supplemented with 5.45 M (319 g/liter) NaCl and incubated at 37°C for 2 h. Each sample was then serially diluted up to 10,000-fold in minimal medium, spotted on LB plates, and incubated overnight at 37°C. The numbers of colonies in each 1,000X to 10,000X dilution were then counted. Each assay was performed in duplicate with independent biological replicates.

Genome sequencing and verification. The evolved Hfr-2xSFX− (G1 to G6) and 2xOriT (A1 to A6) isolates, along with the unevolved parental strains, were sequenced to discover the genotype underlying the observed sodium chloride tolerance. Genomic library preparation and sequencing were performed by The Texas A&M Genomics Center for sequencing on the Illumina HiSeq 2500 platform using 100-bp single-end reads. An average of 286-fold coverage was obtained for each isolate. Reads were assembled against the MG1655 reference genome, and each mutant genome was compared to the parental sequences to identify any *de novo* mutations. The approach to mutation verification depended on the type of mutation; 11 single nucleotide polymorphisms (SNPs) and deletions were verified with Sanger sequencing, and other large deletions were verified with junction-specific PCR (see Table S2 in the supplemental material).

Transcriptional analysis. Two biological replicates of A2, A4, G2, G3, G5, and G6 were used for microarray analysis. Two colonies of each strain along with the 2xOriT (A parent) and Hfr-2xSFX− (G parent) were inoculated into glucose minimal medium supplemented with tryptophan and grown overnight at 37°C with shaking. A total of 500 μl of each overnight culture was diluted 50-fold (OD600 ≈ 0.02) into 250-ml baffled flasks containing 25 ml of glucose minimal medium, supplemented with tryptophan and 0.55 M (32 g/liter) NaCl. Samples were grown until reaching an OD600 of approximately 0.5 and were then harvested by rapid filtration (Nalgene) followed by immediate resuspension in 5 ml of RNAlater (Sigma). RNA processing was done as

described previously [84].

Indole and biofilm measurements. The G2, G3, G5, G6, A2, and A4 mutants, along with the Hfr-2xSFX− and 2xOriT parental strains, were grown in M9 medium supplemented with 0.55 M (32 g/liter) NaCl, 0.5% (wt/vol) glucose, and 50 μg/ml tryptophan until reaching stationary phase. Extracellular indole concentrations were measured using standard procedures with Kovac's reagent [85]. Biofilm formation was measured in 96-well plates with 2 biological and 8 technical replicates per strain in either LB or glucose minimal medium supplemented with NaCl (0.55 M, 32 g/liter) and tryptophan using a previously established protocol [86]. Biofilm data are normalized by final biomass density (OD600) and by specific biomass formation of the parental strains.

Microarray data accession number. Microarray data were deposited in the Gene Expression Omnibus (GEO) database under accession number GSE51611.

RESULTS AND DISCUSSION

Evolution under NaCl challenge. Six replicate populations of 2xOriT and Hfr-2xSFX− were subjected to gradually increasing NaCl concentration (0.55 to 0.75 M, 32 to 44 g/liter) over the course of approximately 150 generations. Over this time course, significant fitness improvements were observed in all evolving populations (Fig. 1), indicating the successful selection for osmotolerant mutants in each population. Compared to the observed rates of fitness improvement in the 2xOriT populations (4.54 X 10^{-3}/generation), the rates of fitness improvement in Hfr- 2xSFX− populations are significantly larger (6.70 X 10^{-3}/generation, $P < 0.003$, Student's t test). However, it is possible that due to the initial higher sensitivity of Hfr-2xSFX− to NaCl, mutants with larger fitness improvements tended to arise in the sexual populations as a result of stronger selection, leading to an apparent increase in the adaptation rate independent of recombination. Interestingly, mutant isolates from the Hfr-2xSFX− populations tended to have higher relative fitness values than those from the 2xOriT populations, as

discussed below. All populations reached similar phenotypic endpoints by the conclusion of the experiment. No loss of mating competence was observed in the Hfr-2xSFX− populations over the course of the experiment.

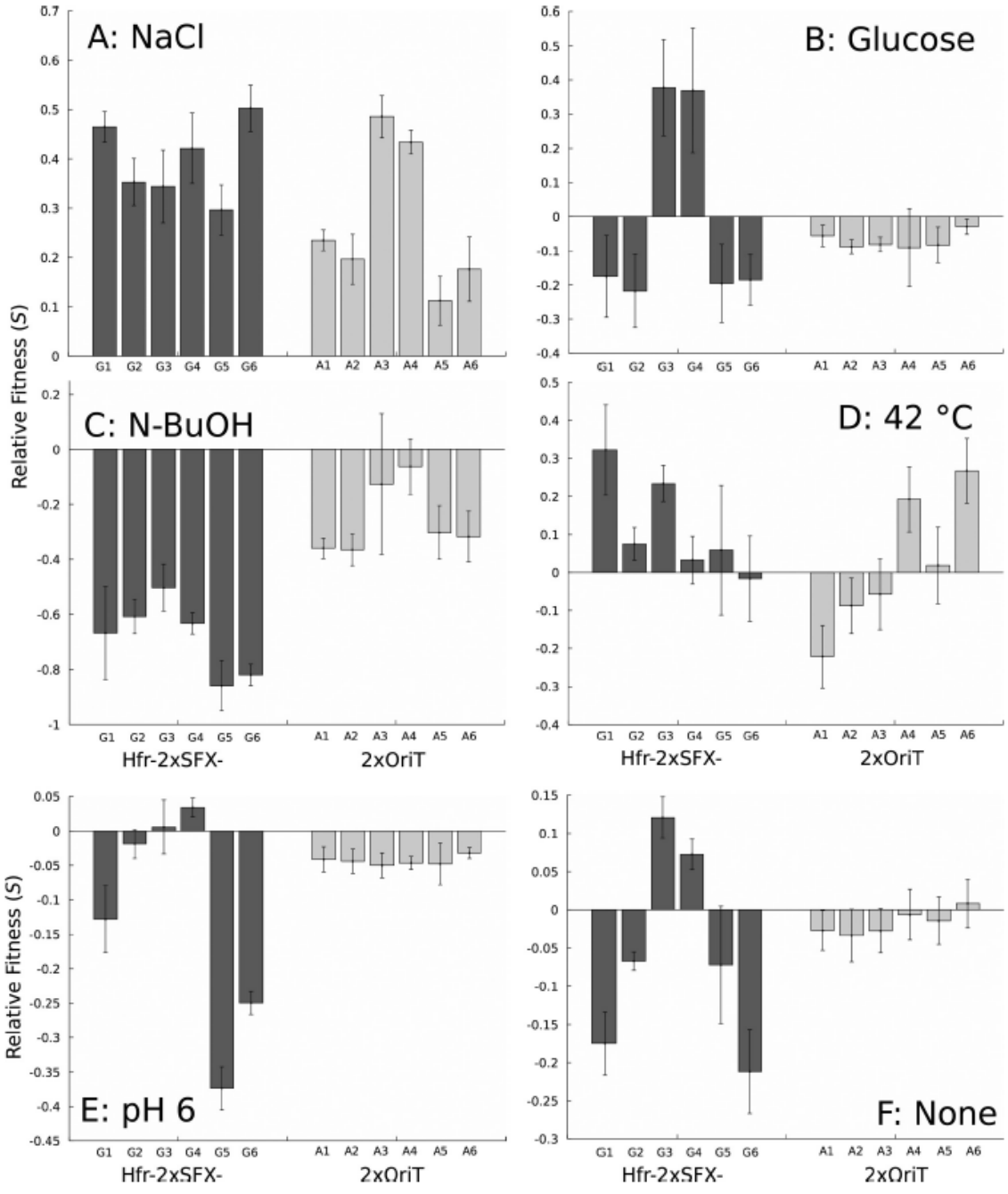

Figure 2. Relative fitness of Hfr-2xSFX− and 2xOriT isolates under several abiotic

stressors, including 0.65 M (38 g/liter) NaCl (A), 0.3 M glucose (B), 0.8% n-butanol (C), growth at 42°C (D), pH 6 (E), and without abiotic stressors (F). Error bars are 95% confidence intervals using the Student t distribution [82].

Mutant characterization. A single randomly isolated clone from each Hfr-2xSFX− (G1 to G6) and 2xOriT (A1 to A6) population was subjected to detailed analyses to identify any novel phenotypes that arose during evolution alongside osmotolerance. All mutants had significant improvements in relative fitness under NaCl challenge (Fig. 2A), though is it possible that mutations that enhance growth in minimal medium [87] are responsible for the apparent tolerance increase. However, only G3 and G4 had significantly improved growth rates in the absence of stress (Fig. 2F). When the observed general fitness benefits in the absence of abiotic stressors were accounted for by calculating mutant relative improvements under NaCl stress (see equation 3), all mutants remained significantly more tolerant than the unevolved 2xOriT strain; these strains likely have acquired mutations beneficial to both growth in minimum medium and in NaCl-challenged conditions. Furthermore, all isolated mutants were capable of growth at 0.80 M (47 g/liter) NaCl, a concentration that completely inhibits growth of the 2xOriT and Hfr-2xSFX− parent strains. In light of the improved NaCl tolerance of the mutants, we also examined their ability to withstand prolonged shocks under hyperosmotic conditions (5.45 M, 319 g/liter NaCl). While most mutants had no improvements in survival relative to 2xOriT under these conditions (data not shown), G3 and G6 rapidly lost viability, exhibiting a 10-fold or more decrease in shock tolerance. It is possible that survival under extreme NaCl concentrations versus growth at lower concentrations requires divergent tolerance mechanisms.

Osmotic tolerance and other complex phenotypes. Resistance to osmotic stress is known to affect other phenotypes of industrial interest, such as *n*-butanol or low pH tolerance [76, 88] and growth at elevated temperatures [89]. Growth assays of the mutants in the presence of inhibitory levels of glucose, 0.8% *n*-butanol, mild acidic pH, and thermal stress (Fig. 2B to E) revealed that the observed tolerance phenotypes are

mostly specific to NaCl resistance alone. The G3 and G4 isolates exhibited increased tolerance of stress-inducing glucose concentrations [69]. Glucose and thermal tolerance levels of the other isolates were generally similar to or slightly below that of the wild-type reference, so it is unlikely that there is a fundamental incompatibility between osmotic tolerance and these phenotypes in general. The acid tolerance of the mutants varied widely for the Hfr mutants, with G5 and G6 exhibiting large (25 to 37%) declines in fitness even under mildly acidic pH. Significant but small decreases in relative fitness under acid stress were also observed in all A mutants. These results imply that there is some degree of antagonistic pleiotropy between tolerance of high osmotic pressures and acid stress, but additional investigation is needed to confirm this hypothesis.

Interestingly, no isolate had improved *n*-butanol tolerance in this case, contrary to previous examples of *n*-butanol-osmotic stress cross-adaptation[62, 76]. The reasons for this apparent incompatibility are unclear, especially given that Dragosits et al. observed a slightly increased level of *n*-butanol tolerance in an isolate evolved under continuous 0.3 M NaCl stress [76]. Stronger NaCl selection could disfavor mutations that also improve *n*-butanol resistance, as it is reasonable to expect that different levels of osmotic stress select for distinct tolerance mechanisms. *n*-Butanol tolerance is also not always associated with improved osmotic stress resistance in evolved mutants [88], so there are at least some evolutionary paths on both the NaCl and *n*-butanol landscapes that lead to divergent tolerance phenotypes. The overall lack of significant cross-adaptation for the isolates in this case does indicate that specialist mutants with adaptations specific only to NaCl tolerance are favored under these evolutionary conditions.

Genetic patterns of adaptation. In order to better understand the genetic bases for the observed osmotolerance phenotypes and to compare tolerance mechanisms between the sexual and asexual populations, we sequenced the genomes of A1 to A6 (2xOriT parent) and G1 to G6 (Hfr-2xSFX− parent) isolates. A complete list of mutated genes, their putative functions, and the structure of each mutation in the isolates is given in Table 1. Many isolates (8/12) harbor likely inactivating frameshift mutations or large deletions

within the *N-acetylglucosamine* (NAG) catabolic operon (nag), either in the gene encoding the transcriptional repressor *nagC* or the deacetylase *nagA.* Amino sugar catabolism may therefore have been altered in these strains. Although this adaptation has not been previously observed in strains evolved under continual osmotic stress, NAG forms a crucial component of peptidoglycan [90], and it is readily conceivable that adaptation to high osmotic stress would involve alterations to cell wall biosynthesis or peptidoglycan recycling. Mutations affecting glucosamine-6-phosphate biosynthesis have also been identified in evolved isobutanol-tolerant *E. coli* [71], so this may be a common mechanism of adaptation to certain membrane-disrupting environmental conditions. Mutants A1, A2, and A3, all containing mutations in *nagA,* were unable to metabolize NAG as a sole carbon source as expected [91]. G4 unexpectedly failed to grow as well, despite the fact that the strain harbors no mutations affecting NAG genes; it is possible that this strain has a large genomic rearrangement affecting *nagA* expression that was not detected in our analysis.

Table 1. Mutations identified with genome sequencing [82].

TABLE 1 Mutations identified with genome sequencing[a]

Strain	Gene(s)	Function	Type	Location (no. of bp[c])
G1	*nmpC, essD*	Outer membrane protein, holin	SNP	Intergenic
	cadB	Lysine, cadaverine transporter	SNP	A171A
G2	*nagCD*	NAG metabolism	Deletion	Coding (−715)
	yhdP	Unknown	SNP	L318R
G3	*rpoC*[b]	β′ subunit of RNAP	Duplication	Coding (2 × 84)
	treR	Trehalose regulator	SNP	S61S
G4	*rpoC*[b]	β′ subunit of RNAP	Duplication	Coding (2 × 84)
	hisC[b]	Histidine biosynthesis	SNP	T170P
G5	*nagC*	NAG metabolism	Deletion	Coding (−1)
G6	*mrdA*[b]	Penicillin binding protein 2	SNP	Q51L
	rpsA[b]	30S protein S1	SNP	Q421K
	ydjK	Predicted transporter	SNP	P17S
A1	*nagA*	NAG-6P deacetylase	Deletion	Coding (−1)
	bcr	Multidrug efflux transporter	SNP	S8A
A2	*mreB*[b]	Actin homolog	SNP	I336L
	nagA	NAG-6P deacetylase	Deletion	Coding (−1)
A3	*mreB*[b]	Actin homolog	SNP	T171S
	nagA	NAG-6P deacetylase	SNP	A203E
	proV	Glycine betaine transporter	IS1	Coding (+9)
	msrB	Methionine sulfoxide repair	SNP	C118F
	fimA	Fimbriae A	IS186	Coding (+6)
A4	*nagCD*	NAG metabolism	Deletion	Coding (−1,570)
	proV	Glycine betaine transporter	IS1	Coding (+4)
A5	*yejM*[b]	Predicted hydrolyase	Duplication	Coding (2 × 9)
	nagC	NAG metabolism	Deletion	Coding (−2)
	mreB[b]	Actin homolog	SNP	S185F
	fimA	Fimbriae A	IS186	Coding (+6)
A6	*nagC*	NAG metabolism	Insertion	Coding (+1)
	mreB[b]	Actin homolog	SNP	K96Q
	bglB	Phospho-β-glucosidase	Deletion	Coding (−1)
	yobF, yebO	Stress, predicted protein	SNP	Intergenic

[a] List of mutations found in each strain (G1 to G6, A1 to A6) relative to their respective parental genotypes. NAG, *n*-acetylglucosamine.
[b] Known essential genes (in general and in glucose minimal medium supplemented with tryptophan specifically). The *rpoC* duplication in G3 and G4 duplicates amino acids 370 to 396 (KKMALELFKPFIYGKLELRGLATTIKA) in domain 2 of the protein (38).
[c] The number of base pairs corresponding to the mutation (e.g., +9 indicates 9 bp added, −1 indicates 1 bp deleted, and 2 × 84 indicates a duplication of 84 bp).

Besides alterations in NAG metabolism, genes encoding cell shape regulators are frequently mutated in the evolved strains. Nonsynonymous SNPs in the cell shape-regulating actin homolog *mreB* [92] and the peptidoglycan transpeptidase *mrdA* genes [93] were identified in five different mutants, suggesting that changes in cell morphology might also reduce osmotic stress on the cell. Microscope examination of the affected strains showed neither a gross difference in cell shape compared to parental controls (data not shown) nor abnormal filamentation, so the precise effect of these

mutations remains unclear. Coincidentally, a previous study examining *mreB* and *mrdA* mutations that suppressed an abnormal shape phenotype caused by RodZ deficiency [94] detected an identical SNP in *mrdA,* implying that RodZ activity may also be deficient under osmotic stress. It is difficult to speculate on how *nag* and *mreB* mutations might interact in the A1, A2, A5, and A6 mutants, as they affect related but distinct cellular processes; changes in *mreB-chromosomal* interactions may result in altered cell division or chromosomal segregation, which may in turn affect the amount of NAG precursor generated from peptidoglycan recycling. Given the seeming ubiquity of mutations affecting both pathways, it is clear that perturbation of cell shape proteins or peptidoglycan metabolism is important for osmotic tolerance.

While both groups of mutants had similar mutation rates (see Materials and Methods), transposon insertions in *fimA* (type I fimbriae) and *proV* (the ATP binding cassette for the *proVXW* glycine betaine transporter) were observed only in the A strains. Fimbrial components, including *fimA,* are highly upregulated under osmotic stress [95], and a mutation that inactivates *fimA* presumably results in conservation of carbon and energy. The relationship between *nagA, nagC,* and surface fiber expression may also play a role in the fitness benefit of *fimA* inactivation, as the *fimA* insertions in A3 and A5 are associated with *nag* mutations as well. The inactivation of *proV* is more peculiar, given its extensively studied role in importing osmoprotectants into the cell [96]. Nonsense mutations affecting *proV* have been previously observed in osmotolerant mutants [76], providing additional evidence that *proV* is under negative selection in hyperosmotic glucose minimal medium.

Mutations in several other genes, while not specifically known to affect osmotic tolerance, were also detected. G1 exhibited both a synonymous mutation in the *cadB* lysine transporter and an intergenic SNP between *nmpC* (an outer membrane protein associated with peptidoglycan) and *essD,* a holin for the integrated prophage DLP12. The latter gene has been shown to be important for cell wall maintenance and biofilm formation [97], which may explain the distinct mechanism behind G1's osmotic

tolerance. G3 and G4 were found to have an 84-bp in-frame duplication (amino acids 370 to 396) within the *rpoC* subunit of RNA polymerase. The duplications occur in region 2 of the protein, which is responsible for RNA polymerization [98]. Due to the role of *rpoC* in promoter recognition and sigma factor binding [99], this mutation should result in significant transcriptional and ultimately phenotypic alterations. Mutations in *rpoC* (along with *rpoB)* have been observed previously in other long-term evolution studies [87] as well, indicating that a wide range of phenotypes can be improved via alteration of RNA polymerase components. A small in-frame duplication was also observed in the essential but un- characterized hydrolase gene *yejM,* but the effect of this mutation is unclear. A range of SNPs in intergenic regions and the coding sequences of various other genes were also detected, including a synonymous substitution in *treR,* a negative regulator of trehalose biosynthesis, in G3 and the S6 ribosomal protein *rpsA* in G6. Other mutations of ribosomal proteins have been found to confer salt tolerance as well [100] by impairing ribosome maturation, but further investigation is needed to understand the functional consequences of this particular point mutation.

In order to better understand the effect of these mutations on osmotolerance, we performed three tests to quantify the fitness effect of gene overexpression, compensation, and knockout on an unaltered host strain (BW25113) and the isolated evolved mutants. Eleven genes (*nmpC*, *yobF*, *ydjK*, *mreB*, *fimA*, *nagC*, *nagA*, *proV*, *treR*, *ydhP*, and *cadB*) were selected for overexpression studies due to their frequency of mutation or nearby intergenic or synonymous SNPs (results shown in Fig. 3A). Of all genes tested, only *ydjK* overexpression conferred a statistically significant improvement in osmotolerance. YdjK is annotated as a putative metabolite transporter, and due to the inclusion of tryptophan in the evolution medium, we reasoned that it might be an uncharacterized tryptophan transporter. However, YdjK did not confer a benefit in the absence of stress ($P = 0.25$, Student's *t* test), so its true function remains unclear. Overexpression of *proV*, *nagC*, or *nagA* is also somewhat deleterious under these growth conditions, though *fimA*, which underwent transposon insertions in several independent mutants, did not have a significant effect on host fitness under these conditions.

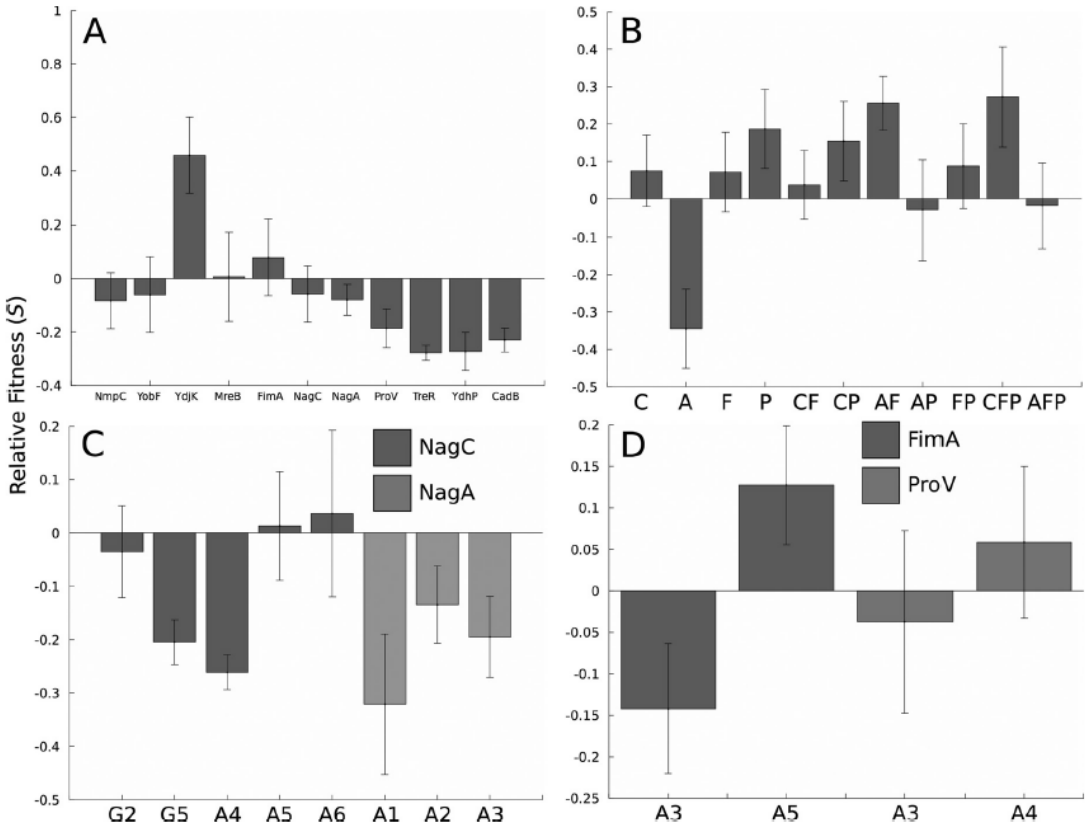

Figure 3. Batch growth screening of overexpression, knockout, and compensatory strains to identify their osmotolerance phenotypes in glucose minimal medium supplemented with 0.55 M NaCl. (A) Fitness of overexpression strains relative to the empty vector pCA24N control. Only ydjK expression results in a significant tolerance improvement. (B) Fitness of knockout strains relative to BW25113; strain genotypes are denoted as follows: C, ΔNagC; A, ΔNagA; F, ΔFimA; and P, ΔProV. (C) Overexpression of NagC and NagA in mutants with possibly inactivating mutations in these genes; fitness is relative to the corresponding mutant with pCA24N. (D) Overexpression of FimA and ProV in mutants with possibly inactivating mutations in these genes, with the empty vector as a reference. All error bars are 95% confidence intervals based on the Student distribution [82].

Likely inactivating mutations in a small set of genes, including *nagC*, *nagA*, *fimA*, and *proV*, were identified in several of the G and A mutants. Various combinations of these

mutations were found in the evolved mutants, suggesting the presence of potential epistatic interactions that affect osmotic tolerance. We tested this hypothesis by systematically reconstructing double and triple mutants containing defined *nagA* or *nagC* disruptions, along with knockouts in *fimA* and *proV*. Figure 3B shows the relative fitness of these knockout mutants versus an unmodified BW25113 strain. Of the single mutants, only the *proV* strain is fitter than the reference. Interestingly, the *nagA* knockout has a large negative impact on strain fitness, suggesting that the insertion and deletion mutations identified in the sequenced mutants were not completely inactivating or the inactivation of *nagA* has a positive synergistic effect with other mutations in these mutants. As potential evidence for the presence of synergistic interactions between mutations, double knockouts of *nagC* and *proV* or *nagA* and *fimA* were found to be beneficial in the presence of NaCl challenge. Only the *nagC fimA proV* triple mutant showed improved osmotolerance relative to BW25113. These combinations did not occur in any mutant, and it is possible structural differences between the defined knockouts and mutations in the osmotolerant isolates could also influence these results. Overall, as was the case with overexpression analysis, these results indicate that these four genes affect the *E. coli* osmotolerance phenotype.

An additional way of confirming that the mutations in *nagA*, *nagC*, *proV*, and *fimA* play a role in modulating osmotolerance is to complement the mutations in *trans* with an expression plasmid and then reassay their fitness under osmotic stress. The results of this test are shown in Fig. 3C and D and indicate that the effect of compensation depends heavily on the genetic background of the particular mutant. Relative fitness of only two *nagC* mutants (G5 and A4) out of five is decreased by *nagC* overexpression, while *nagA* complementation decreased osmotic tolerance of A1 to A3. The structure of the *nagC* mutations does vary significantly between the mutants, which may explain the lack of concordance in complementation results. Complementing the *proV* mutations in A3 and A4 had no significant fitness effect. While *fimA* overexpression decreased the fitness of A3, it also improved the fitness of A5 slightly, despite their identical IS186 insertions into the gene. It is likely that genetic differences between the various mutants and

interactions between other mutations not screened in this assay also play a significant role in determining the fitness impact of gene complementation.

Though genome sequencing has revealed several novel loci involved with osmotolerance, the genotype-phenotype relationship remains unclear. To gain a more complete understanding of how these mutations translate into improved osmotic stress tolerance, we applied microarray technology to several A and G mutants with distinct underlying mutations to identify transcriptional perturbations that may result from their underlying mutations or altered stress responses.

Mutation-induced transcriptional perturbations. Six sequenced mutants, G2, G3, G5, G6, A2, and A4, were selected for transcriptomic analysis based on their distinct underlying genotypes and varied levels of osmotolerance and therefore are likely to have diverse tolerance mechanisms. Genes commonly upregulated in these mutants, along with those representing possibly novel mechanisms, are listed in Table 2. The gene encoding AcrZ, a small protein associated with the AcrAB-TolC efflux pump complex known to affect AcrB substrate recognition [101], is upregulated in all mutants except A4, suggesting that it may be an important transcriptional adaptation. Sulfonate transport and metabolism genes (*tauABC*, *ssuEADC*) are also frequently upregulated in the mutants. Ordinarily, these proteins are intended to scavenge sulfur from the environment, but under osmotic stress, they can also import osmoprotectants such as taurine [102]. This upregulation cannot be explained as simple sulfur starvation, as the mutants and references were in exponential growth before RNA harvesting. The *proVXW* operon, positively regulated by hyperosmotic conditions [103], is also overexpressed by G3 and G5, though *proX* and *proW* are also overexpressed in A4, G3, G5, and G6. This expression pattern may explain the fitness benefit of *proV* deletion found in A3 and A4 in terms of energy conservation, as discussed previously.

Table 2. Overexpressed genes of interest [82].

TABLE 2 Overexpressed genes of interest[a]

Gene	COG[b]	Function	Strain(s)
acrZ		Cell envelope stress response	A4, G2, G3, G5, G6
ssuD	C	Alkanesulfonate monooxygenase	G2, G3, G5, G6
proV	E	Glycine betaine transporter subunit	G3, G5
proW	E	Glycine betaine transporter subunit	A4, G6
proX	E	Glycine betaine transporter subunit	A4, G3, G5, G6
tnaA	E	Tryptophanase/L-cysteine desulfhydrase	G2, G3, G5, G6
tnaB	E	Tryptophan transporter of low affinity	G2, G3, G6
entC	HQ	Isochorismate synthase 1	G3
acs	I	Acetyl-CoA synthetase	G5, G6
ymdC	I	Cardiolipin synthase 3	G2
fabF	IQ	3-Oxoacyl-[acyl carrier protein] synthase II	G6
nagC	KG	Repressor of NAG operon	A4, G2
arnC	M	Undecaprenyl phosphate-L-Ara4FN transferase	A2, A4
lpp	M	Murein lipoprotein	A2, A4, G2, G3
ompA	M	Outer membrane porin A	G2
ompC	M	Outer membrane porin C	G2, G3, G5, G6
ompG	M	Outer membrane porin G	A2, A4
ompL	M	Outer membrane porin L	A2, A4
ompX	M	Outer membrane protein X	A2, A4, G3, G5
feoB	P	Fused ferrous iron transporter	G5
fepG	P	Iron-enterobactin transporter subunit	G5
fiu	P	Catecholate siderophore receptor Fiu	G3
ssuA	P	Putative aliphatic sulfonate binding protein	G2, G3, G5
ssuC	P	Putative alkanesulfonate transporter subunit	A2, A4, G2, G3, G6
tauA	P	Taurine transporter subunit	G3, G6
tauB	P	Taurine transporter subunit	G2, G3, G6
tauC	P	Taurine transporter subunit	A4, G2, G3, G5, G6
entE	Q	Enterobactin synthase complex component	G3
entF	Q	Enterobactin synthase complex component	G3, G5
entH	Q	Thioesterase for efficient enterobactin production	G3
tauD	Q	Taurine dioxygenase, 2-oxoglutarate dependent	G3, G6
fadM	R	Long-chain acyl-CoA thioesterase III	G2, G3, G6
ssuE	R	NAD(P)H-dependent FMN reductase	G2, G3, G5, G6
ydcH	S	Predicted protein	G2, G3, G5, G6
yodC	S	Predicted protein	G2, G3, G5, G6
csrA	T	Carbon source metabolism regulator	G2, G3, G5

[a] Overexpressed genes of interest for A2, A4, G2, G3, G5, and G6 as identified with microarray analysis. The overexpression of all genes listed here is statistically significant at a *P* value of ≤0.01. A complete list of overexpressed genes for all strains and their expression ratios is given in Table S3 in the supplemental material. CoA, coenzyme A.
[b] COG, cluster of orthologous groups.

Though the 2xOriT and Hfr-2xSFX− parental strains are for the most part isogenic, the latter is a tryptophan auxotroph due to insertion of the *tra* operon into the *trp* locus [77]. These four G strains all exhibited overexpression of the genes encoding the tryptophan transporter *tnaB* and tryptophanase *tnaA*, which converts tryptophan into indole and pyruvate, as has been previously observed in medium containing tryptophan [104]. Indole is a potent signaling molecule involved with various aspects of biofilm and cell cycle regulation [105], so the physiological effect of excess indole is likely to be complex. G2, G5, and G6 exhibit statistically significant increases ($P < 0.05$, Student's *t* test) in indole accumulation compared to the Hfr-2xSFX− parent (Fig. 4) under osmotic stress. A4 produces significantly less indole ($P < 0.045$,Student's *t* test) than its 2xOriT

ancestor as well. Despite the fact that G3 has roughly equivalent upregulation of *tnaA* transcription to these strains, indole production is similar to that of the wild type; it could be that the unusual in-frame duplication in *rpoC* in this strain results in increased *tnaA* transcription, but the resulting mRNA is poorly translated into protein or degraded rapidly due to posttranscriptional regulation.

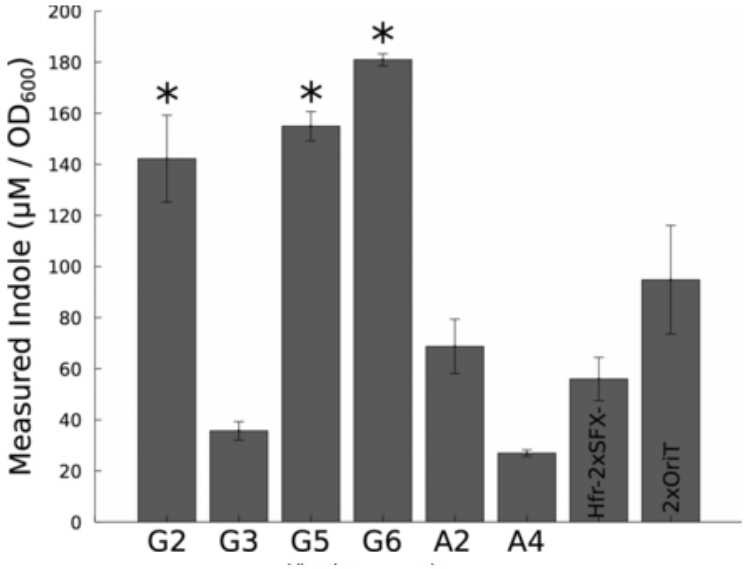

Figure 4. Levels of indole, normalized by biomass density, for G2, G3, G5, G6, A2, and A4 mutants, along with the G parent Hfr-2xSFX− and A parent 2xOriT. Error bars are standard deviations. G2, G5, and G6 (with asterisks) have statistically significant increases in indole accumulation compared to Hfr-2xSFX− ($P < 0.05$, Student's t test) [82].

Due to the intertwined nature of indole and biofilm regulation, we also examined the biofilm formation propensity of the evolved mutants. Most G and A mutants under osmotic stress form significantly less biofilm than their ancestral parents (Fig. 5), though G mutants typically had larger decreases than the A strains. Perturbations in the *nag* pathway may play a role in modulating biofilm formation, as both *nagA* and *nagC* deletions have been shown to affect surface fiber synthesis, including curli [106] and fimbriae [107], due to the accumulation of intracellular NAG-6-phosphate. Given the

large number of detected mutations that may affect biofilm formation or cell wall properties, this evolutionary route for tolerance improvement clearly warrants further research to better understand selection pressures on biofilm synthesis.

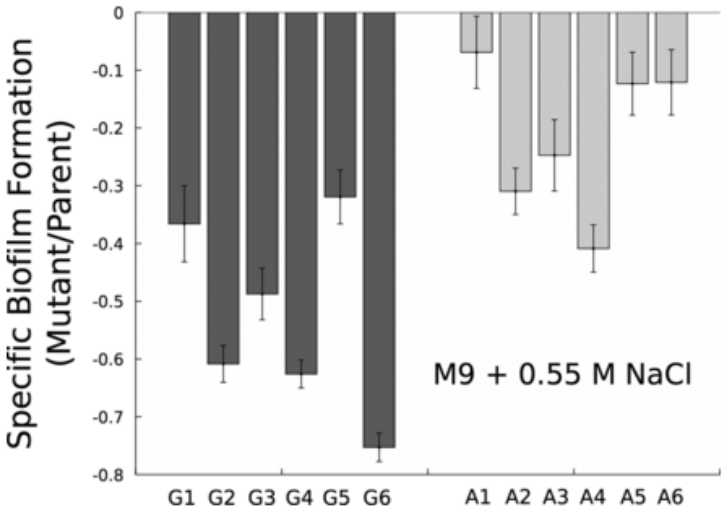

Figure 5. Relative biofilm formation by G1 to G6 and A1 to A6 mutants in glucose minimal medium with 0.55 M (32 g/liter) NaCl. Data are ratios of mutant-specific biofilm formation to parental formation (G, Hfr-2xSFX−; A, 2xOriT) under these conditions. Data are normalized by biomass yield (OD600). Error bars are 95% confidence intervals [82].

Beyond metabolite transporters, several genes involved with iron uptake (*entCEFH*, *feoB*, *fepG*, *fiu*) were overexpressed in G3 and G5 as well. Increased expression of iron transport and metabolism genes has been found in evolved mutants with improved osmotic or *n*-butanol tolerance[62, 76]. Perturbation of iron metabolism may therefore be a contributor to osmotic tolerance, though the gene encoding the siderophore receptor *fiu* is also downregulated in G2 and G6. Genes involved in membrane composition were also upregulated in many mutants, particularly certain outer membrane porins (*ompACGL*) along with the *ompX* gene. These transcriptional disturbances may represent an attempt by the mutants to change membrane-sieving properties in order to reduce osmotic pressure on the cell. The peptidoglycan-outer membrane tether gene, *lpp*

(murein lipoprotein), was also overexpressed in four different mutants (A2, A4, G2, G3), which may indicate that the peptidoglycan wall is more strongly attached to the outer membrane in these mutants to protect the cell against high external osmotic pressure. Several genes that encode hypothetical or predicted proteins (*ydcH*, *yodC*) are consistently overexpressed in the G mutants, but no information about their biochemical roles or relationship with osmotolerance is known.

In contrast to the relative similarities in gene overexpression under osmotic stress between these six mutants, less similarity is observed for genes repressed relative to the parental references (Table 3). The few commonly repressed genes include those coding for several hypothetical or conserved proteins (*yegR*, *ydeMN*, *rtcB*) and the transcriptional activator *ydeO*, known to regulate acid resistance in concert with EvgA [108]. Their repression may be associated with the reduced osmotic stress experienced by the mutants compared to that of their parents under these conditions, as these genes are not known to be directly regulated by osmotic stress. Downregulation of several siderophores and enterobactin transporters was observed in G2, G5, and G6, including *fepA*, which was found to be strongly overexpressed in a previously evolved osmotolerant *E. coli* strain [76].

Table 3. Repressed genes of interest [82].

TABLE 3 Repressed genes of interest[a]

Gene	COG[b]	Function	Strain(s)
yegR		Predicted protein	A4, G2, G, G5, G6
rfaZ		Lipopolysaccharide core biosynthesis protein	A2, A4
nagB	G	Glucosamine-6-phosphate deaminase	A4, G2, G3, G5
nagE	G	NAG PTS enzyme: IIC, IIB, IIA components	G2, G3, G5
nagA	G	*N*-Acetylglucosamine-6-phosphate deacetylase	G2, G3
fabD	I	Malonyl-CoA-[acyl carrier protein] transacylase	G6
ydeO	K	Transcriptional activator for *mdtEF*	G2, G3, G5, G6
rpoB	K	RNA polymerase, β subunit	A2, A4
rpoC	K	RNA polymerase, β′ subunit	A2, A4
rpoE	K	RNA polymerase, σ^E factor	A2, A4
fimB	L	FimA promoter invertase	G6
bamC	M	Lipoprotein required for OM biogenesis	A2, A4
kdsB	M	3-Deoxy-manno-octulosonate cytidylyltransferase	A2, A4
mltD	M	Predicted lytic murein transglycosylase D	A2, A4
murC	M	UDP-*N*-acetylmuramate:L-alanine ligase	A2, A4
murI	M	Glutamate racemase	A2, A4
ompF	M	Outer membrane porin 1a (Ia;b;F)	G3, G6
wbbK	M	Lipopolysaccharide biosynthesis protein	A2, A4
acrA	M	Multidrug efflux system	G6
acrE	M	Cytoplasmic membrane lipoprotein	G5
amiB	M	*N*-Acetylmuramoyl-L-alanine amidase II	A4
flgJ	MNO	Muramidase	G5
fimC	NU	Chaperone, periplasmic	G5, G6
fimA	NU	Major type 1 subunit fimbrin (pilin)	G6
fimD	NU	Puter membrane usher protein	G5
fimG	NU	Minor component of type 1 fimbriae	G5
fimI	NU	Type 1 pilus biosynthesis protein	G6
ydeN	P	Conserved protein	A2, A4, G3, G5
fiu	P	Catecholate siderophore receptor Fiu	G2, G6
cirA	P	Catecholate siderophore receptor CirA	G6
efeO	P	Inactive ferrous ion transporter EfeUOB	G6
fecD	P	Iron-dicitrate transporter subunit	G5
fepA	P	Iron-enterobactin outer membrane transporter	G6
ydeM	R	Conserved protein	G2, G3, G5
rtcB	S	Conserved protein	G3, G5, G6

[a] Repressed genes of interest for A2, A4, G2, G3, G5, and G6. The repression of all genes is statistically significant at a *P* value of ≤0.01. A complete list of repressed genes for all strains and their expression ratios is given in Table S3 in the supplemental material. CoA, coenzyme A.
[b] COG, cluster of orthologous groups.

As was the case for upregulated genes, repression of genes involved with peptidoglycan and membrane biosynthesis was significantly enriched in the mutant transcriptomes according to gene ontology analysis. NAG catabolism genes, *nagA*, *nagB*, and *nagE*, were repressed in A4 and several G mutants. Repression of many other peptidoglycan or outer membrane-related genes was observed in A2 and A4, particularly those genes involved with cell wall maturation (*mltD*, *murC*) or lipopolysaccharide synthesis (*rfaZ*, *kdsB*, *wbbK*). Membrane remodeling therefore appears to be a significant adaptive response in these mutants. Fimbriae synthesis and assembly genes were also repressed in G5 and G6, lending credence to the hypothesis that *fimA* inactivation may be part of an energy conservation response during laboratory evolution. Porin synthesis also is

perturbed in G3 and G6 by simultaneous repression of *ompF* and overexpression of *ompC*, as is typically observed under high osmotic pressure [109]. The totality of these transcriptional responses point to wide-ranging changes in gene expression affecting membrane composition, transport activity, iron metabolism, and other systems stemming from various underlying genetic changes, to alleviate osmotic stress in these mutants.

Comparison of sexual, asexual adaptation. Evolving populations are generally genetically heterogeneous and therefore contain competing mutant lineages that have arisen independently. Clonal interference will generally reduce this diversity, possibly resulting in a more narrow distribution of mutant fitnesses within asexual populations. To test this hypothesis, we isolated random clones from the Hfr-2xSFX− and 2xOriT populations to evaluate the degree of fitness heterogeneity within each population and to determine whether horizontal gene transfer had a detectable effect on the population structure. The fitness distributions for these populations, shown in Fig. 6, show that Hfr-2xSFX− lines tended to have a slightly higher mean relative fitness but with significantly more variance than the 2xOriT replicates at a high level of significance (P =1.81 X10^{-4}, Kolmogorov-Smirnov test). Genetic diversity within Hfr-2xSFX− lines may therefore be greater than that of the 2xOriT populations; a likely explanation is that horizontal gene transfer reduces the extinction of beneficial clones due to clonal interference and drift, resulting in a maintenance of heterogeneity that is less likely to occur in an asexual population [110, 111]. However, as all populations reached similar fitness endpoints during the experiment, further adaptation beyond that observed here could be mutation limited.

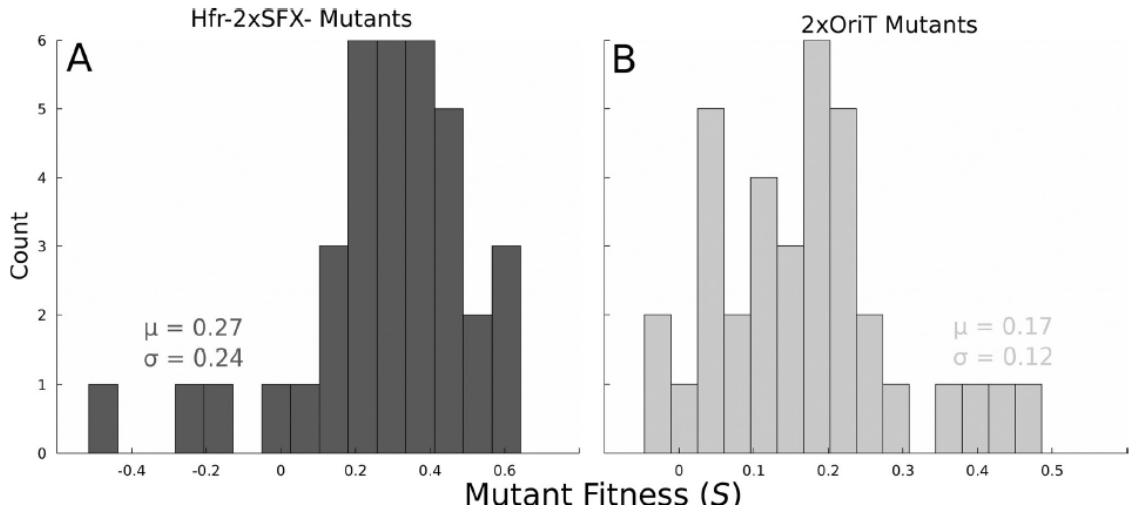

Figure 6. Histogram of relative fitness (to 2xOriT) in randomly screened isolates from six Hfr-2xSFX− (A) and 2xOriT (B) populations. All isolates were challenged with 0.65 M (38 g/liter) NaCl. Differences in the underlying fitness distributions in the Hfr-2xSFX− and 2xOriT populations are highly significant (P = 1.81 × 10−4, Kolmogorov-Smirnov test) [82].

In an attempt to further improve the observed NaCl tolerance levels of the mutants, we performed a short-term mating experiment where the G1 to G6 isolates were mixed together to facilitate genetic transfer and then propagated under NaCl selection for 5 days. Surprisingly, analysis of clonal isolates from the mixed G population revealed that the fittest clones were no better than the original fittest Hfr-2xSFX− mutant G6 (data not shown). Genome sequencing revealed that many of the G mutants have mutations in close proximity or actually overlapping in the case of the independent *nagC* mutations. Recombination events capable of combining these genotypes may therefore be rare. Negative epistasis between other mutations may have also prevented successful generation of recombinants.

Conclusions. These results provide new insight into the *E. coli* osmotolerance phenotype. All isolates exhibited high levels of osmotolerance as expected, and a surprising lack of cross-adaptation to other stressors, such as excess glucose, *n*-butanol,

low pH, and thermal stress. Genomic sequencing revealed novel mutations in genes related to *n*-acetylglucosamine catabolism, cell shape regulation, uptake of osmoprotectants, and global regulators such as *rpoC*. Many of the mutations occurred in genes known to affect cell wall or peptidoglycan maintenance. On a transcriptional level, membrane and peptidoglycan synthesis, porin expression, sulfonate uptake, and iron metabolism are all significantly perturbed in various evolved mutants relative to their parental references and might be targets of interest for future studies of this phenotype. Future work will continue to explore the transcriptomic data in hopes of identifying additional loci influencing osmotic tolerance, in addition to reconstructing the observed mutations in the A and G isolates in industrial *E. coli* strains to improve their osmotolerance under industrial conditions.